Performance of Space-Time Trellis Codes in Fading Channels

by

Mohammad Omar Farooq
B.Sc., University of Dhaka, Bangladesh, 1999
M.Sc., University of Dhaka, Bangladesh, 2001

A Thesis Submitted in Partial Fulfillment of the Requirements for the Degree of

MASTER OF APPLIED SCIENCE
in the Department of Electrical and Computer Engineering

Supervisor: Dr. T. Aaron Gulliver

ABSTRACT

One of the major problems wireless communication systems face is multipath fading. Diversity is often used to overcome this problem. There are three kind of diversity - spatial, time and frequency diversity. Space-time trellis coding (STTC) is a technique that can be used to improve the performance of mobile communications systems over fading channels. It is combination of space and time diversity. Several researchers have undertaken the construction of space-time trellis codes. The Rank and Determinant Criteria (RDC) and Euclidean Distance Criteria (EDC) have been developed as design criteria.

In this thesis we presented evaluation and performance of the Space-Time Trellis Codes (STTC) obtained using these design criteria over Rayleigh, Ricean and Nakagami fading channels. Our simulation results show that the 4,8,16 and 32-state codes designed using the EDC perform worse than the codes designed using RDC in a system with two transmit antennas and a single receive antenna over Nakagami fading channels. But for two transmit antennas and multiple receive antennas the codes designed using the EDC outperforms the codes designed using the RDC. This trend in performance was also observed over Rayleigh fading channels. The results presented in this thesis show that the RDC and EDC design criteria are suitable for both independent and correlated Nakagami fading channels.

Table of Contents

List of Tables

List of Figures

List of Abbreviations

AWGN	Additive white Gaussian noise
BER	Bit error rate
BPSK	Binary phase shift keying
dB	Decibel
EDC	Euclidean Distance Criteria
FFC	Feed forward convolutional code
LSB	Least significant bit
LoS	Line of sight
MIMO	Multiple input multiple output
MSB	Most significant
NLoS	Non line of sight
OFDM	Orthogonal frequency division multiplexing
PDF	Probability density function
PSK	Phase-shift-keying
QAM	Quadrature amplitude modulation
QoS	Quality of service
RDC	Rank and determinant criteria
SNR	Signal to noise ratio
STBC	Space-time block code
STC	Space-time code
STTC	Space-time trellis code

Acknowledgement

I would first like to express my gratitude towards my supervisor, Professor T. Aaron Gulliver without whose guidance, attention to detail and encouragement, I could not have completed this work. I would also like to thank my parents, who have always given me their support and encouragement in my various endeavours. I want to thank my elder brother and sisters for their continuous unconditional love and support in all my life. The friendly and supportive atmosphere inherent to the Communication Group at UVic contributed essentially to the final outcome of my studies. My special thanks goes to my friend Wei Li. I would also like to thank Yousry Abdel-Hamid, Caner Budakoglu, Richard Chen, William Chow, Majid Khabazian and Yihai Zhang. Lastly, I would like to thank all of my friends in UVic. They have helped me to make my time here at UVic more enjoyable.

CHAPTER 1
INTRODUCTION

Introduction

Guglielmo Marconi started wireless communication over 100 years ago. Today wireless technology is a vital part of human civilization. This industry is growing very rapidly with a significant increase in the number of subscribers. As a result, the industry is constantly in need of research and development of new technology to produce better performance. There are many challenges a wireless system faces to provide higher data-rates, better quality of service (QoS), fewer dropped calls and higher network capacity. A wireless system designer often faces two major challenges. The first is limited availability of the radio frequency spectrum and the second is a complex time-varying wireless environment i.e., multipath fading. This thesis is concerned with multipath fading and methods to get better performance in this hostile environment.

Multipath fading, which widely changes the signal amplitude, often disturbs wireless communication systems. Better reception can be obtained with more transmit power, but for mobile systems power consumption is a major issue. If a handheld device needs less power then the physical dimensions and weight can be reduced which may provide the user with more mobility. The mobile wireless industry is also looking for new technologies to provide more services to an increasing number of subscribers. As the number of customer increases the industry will look to new technologies to provide better service at a cheaper price.

In the case of severe attenuation of the transmitted signal due to fading channels, it becomes impossible for the receiver to determine the transmitted signal unless additional independent replicas of the transmitted signal can be supplied to the receiver. This redundancy is called diversity. This is considered as single most important mechanism for reliable wireless communications. There are several techniques for achieving diversity i.e., frequency diversity, spatial (antenna) diversity and temporal diversity.

Frequency Diversity: Signals transmitted on different frequencies induce different multipath structures. In frequency diversity the information signal is transmitted on more than one carrier frequency. In this way replicas of the transmitted signals are supplied to the receiver in the form of redundancy in the frequency domain.

Temporal Diversity: In temporal (or time) diversity, replicas of the information signal are transmitted in different time slots so that multiple, uncorrelated versions of the signal will be received.

Spatial Diversity (Antenna Diversity): Spatial diversity is one of the most popular forms of diversity used in wireless communication systems. Multiple and spatially separated antennas are employed to transmit or receive uncorrelated signals. Antenna separation should be at least half of the carrier wavelength to ensure sufficiently uncorrelated signals at the receiver.

1.1 Fading Channels

In a wireless communication environment a Non-Line-of-Sight (NLoS) radio propagation path will often exist between the transmitter and receiver because of natural and man-made obstacles situated between the transmitter and receiver. As a result the signal propagates via reflections, diffraction and scattering.

In this thesis we evaluate the performance of Space-Time Trellis Code (STTC) over several types of fading channels (Rayleigh, Ricean and Nakagami fading). A Rayleigh distribution is commonly used in wireless communications to describe the statistical nature of the received envelope of a NLoS fading signal. The Rayleigh distribution has a probability density function (pdf) given by [1]

$$p(\alpha) = \frac{\alpha}{\Omega} \exp\left(-\frac{\alpha^2}{2\Omega}\right) \qquad (\alpha \geq 0) \tag{1.1}$$

where Ω is the total received power. Some types of fading channels have a Line-of-Sight (LoS) component. In this case random multipath components are superimposed on a stationary dominant signal. The distribution of this signal is typically denoted as Ricean. The Ricean pdf is given by

$$p(\alpha) = \frac{(K+1)}{\Omega}\exp\left(-K - \frac{(K+1)\alpha^2}{\Omega}\right) I_0\left(2\sqrt{\frac{K(K+1)\alpha}{\Omega}}\right) \quad for(\alpha \geq 0) \tag{1.2}$$

$I_0(\bullet)$ is the zero-order modified Bessel function of the first kind. The parameter K is known as the Rice factor. It is the ratio of the deterministic specular component (LoS) power s^2 and the scattered signal component power $2b_0$ [1]

$$K = s^2/(2b_0)$$

When K=0, the channel exhibits Rayleigh fading and when $K = \infty$ the channel does not exhibit any fading at all. The Nakagami distribution was introduced by Nakagami [2] to characterize fast fading (channel parameters changes rapidly). It has been found that Nakagami distribution or m-distribution is a more versatile model for rapid fading [3]. In this model we assume that the signal is a sum of vectors with random amplitudes and random phases.

The Nakagami pdf is given by [1]

$$p(\alpha) = \frac{2}{\Gamma(m)}\left(\frac{m^m}{\Omega^m}\right)\alpha^{2m-1}\exp\left\{-\frac{m\alpha^2}{\Omega}\right\} \qquad m \geq \frac{1}{2} \tag{1.3}$$

The Nakagami distribution is identical to the Rayleigh distribution when m=1 and when $m = \infty$ there is no fading and the distribution is Gaussian. One of the interesting features of the Nakagami distribution is that since it is defined for $m \geq 0.5$, a Nakagami fading channel can be worse than a Rayleigh fading channel.

1.2 Diversity and MIMO Channels

As discussed earlier, diversity can be obtained by using multiple antennas in the transmitter and/or the receiver. Multiple-Input Multiple-Output (MIMO) channels, also called correlated parallel channels, are encountered when multiple transmit and receive antenna are employed. If these antennas are separated sufficiently in space we can assume independent fading paths. Figure 1.1 shows the model of a MIMO channel with n_T transmit and n_R receive antennas. The received signal can be described by

$$y_j(t) = \sum_{i=1}^{n_T} h_{i,j} x_i(t) + \eta_j(t) \qquad (1.4)$$

$$j = 1, 2, \ldots n_R$$

where x_i is the complex signals transmitted from the $i-th$ antenna, and y_j is the superposition of the faded signal from all the transmit antenna corrupted by noise η_j at the $j-th$ receive antenna. The noise is complex additive Gaussian noise with variance $N_0/2$ in each dimension.

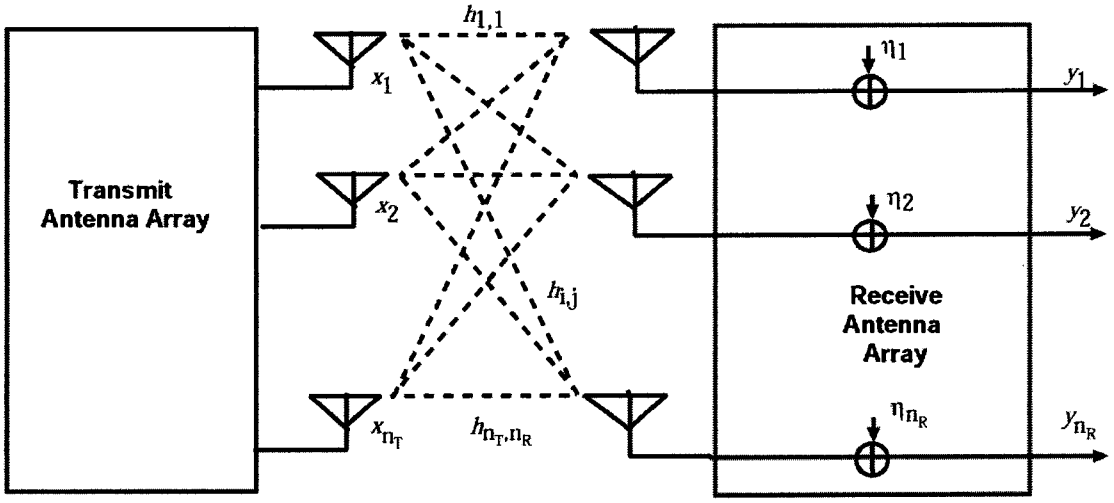

Figure 1.1 MIMO channel Model

1.3 Space-Time Codes

In space-time coding, multiple antennas are used at the transmitter. Coding of symbols across space and time can be employed to yield coding gain and diversity gain. Coding gain is defined as the reduction in signal to noise (SNR) for the same FER that can be realized through the use of a code [4]. Diversity gain performance improvement that can be achieved from a system by using diversity. Figure 1.2 illustrates typical coding gain and diversity gain. The x-axis of the plot is frame error rate (FER) and y–axis is SNR. FER is a commonly used

the measure of the system performance. It is the ratio of the number of erroneous frames of data at the receiver output to the total number of total transmitted frames of data.

Space-Time Codes (STC) were introduced independently by Tarokh et al. [5]-[11] and Alamouti [12] as a novel means of providing transmit diversity for multiple-antenna fading channels. There are two different types of STC. One is as space-time trellis codes (STTCs) and other is space-time block codes (STBCs) [12]. Designing good STTCs is a very complex task, just like designing convolution codes, for which the best techniques involve a search.

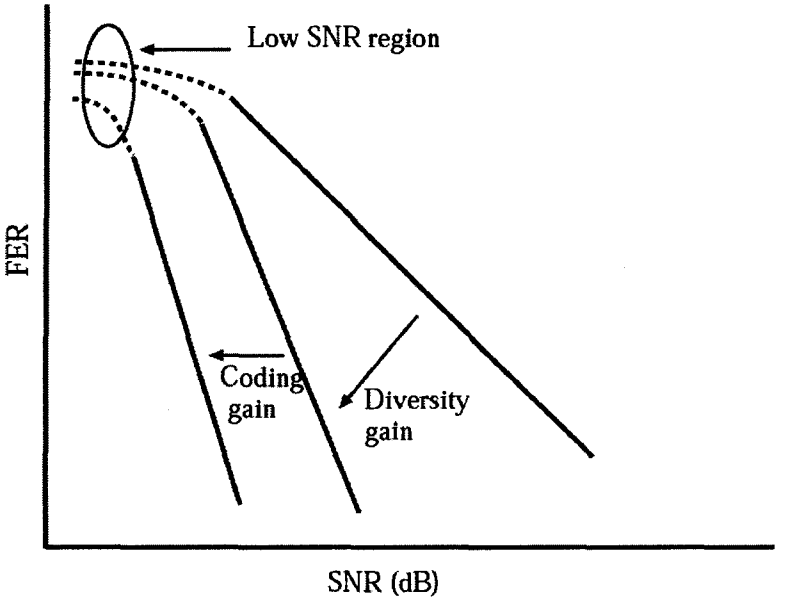

Figure 1.2 Schematic showing coding gain and diversity gain

In addition decoding a STTC is complicated. To reduce the decoding complexity, Alamouti [12] discovered a remarkable scheme for transmitting using two transmit antennas, which is appealing in terms of both simplicity and performance. Tarokh et al. used this scheme for an arbitrary number of transmitter antennas, leading to the concept of space–time block codes (STBC) [10]. STBCs have a fast decoding algorithm. STBCs can be classified into real orthogonal designs and complex orthogonal designs. The former deals with real constellations such as PAM, while the latter deals with complex constellations such as PSK and QAM. Real orthogonal designs have been well developed. In [10], Tarokh et al. proposed systematic constructions of real orthogonal designs for any number of transmit

antennas with full rate. However, complex orthogonal designs are not well understood. There exist several different types of space-time block codes obtained from complex orthogonal designs [11][12][13] [14]. One of the key features the STBCs obtained from orthogonal designs is that by performing linear processing at the receiver data symbols can be recovered. This feature is attractive for mobile and portable communication systems.

The diversity gain obtained from a STTC is equal to the diversity gain from a STBC for the same numbers of transmit and receive antennas. However STTC can also provide coding gain, which a STBC cannot provide. However this additional coding gain is obtained at the cost of increased decoding complexity at the receiver because a Viterbi or trellis based decoder has to be employed. Note that the complexity of the decoder increases with the number of states in the trellis and the number of transmit antennas [15].

1.4 Significance of the Research

As mentioned earlier, STBCs provide diversity gain but no coding gain. On the other hand STTCs have both diversity and coding gain, but the complexity of designing a good code is the main drawback of STTC. There has been rapid progress in this field, targeted at finding better codes with full diversity and with greater coding gain than those provided in [5] and [6]. Baro et al. [16] reported improved STTCs that were found through exhaustive computer search over a feed-forward convolution code (FFC) generator. Ionescu et al. [17] and [18] found improved 8 and 16-state STTCs for 4-PSK for the case of two transmitters in flat Rayleigh fading via a modified determinant criterion. Similarly Chen et al. [19], [20], [21] and [22] derived more accurate code design criteria by using a tighter bound for the $Q(.)$ function in the pairwise error probability (PEP) approximation in [5]. This yielded new STTCs with better performance than the original codes proposed by Tarokh et al. A more structured method of code construction that ensures full diversity is provided in [23], along with a number of new code designs, such as codes that yield the best distance spectrum properties among all codes with a given coding gain [24].

Boleskei et al. [25] considered the effect of receive and transmit correlation in multiple-input-multiple output (MIMO) systems on error performance of STCs. They showed that the resulting maximum diversity order was given by the ranks of the receive and transmit

correlation matrices. Further work has been undertaken to study the performance of STBCs and STTCs and to develop robust codes for correlated fading channels [26].

The work in this thesis concentrates on the performance of the codes proposed in [5] [19] [21] over different fading channels. In this thesis we first present the performance of STTCs over Rayleigh fading channels and then we compare these results with the performance in Ricean and Nakagami fading channels. In [3] the performance of the 4 and 8-state 4-PSK codes proposed in [5] [9] over both independent and correlated Nakagami fading channels was presented. However the performance of the codes proposed by Chen et al. [19][21] have not been investigated over Nakagami fading channels. In this thesis we consider the 4,8,16 and 32-state codes proposed in [5], [19] and [21] over both independent and correlated Nakagami fading channels.

It is very important to investigate code performance over fading channels. In general the Rayleigh and Ricean distributions are frequently used, but the Nakagami distribution is a more versatile fading model [3]. Thus we present more results for this channel. Since a Nakagami fading channel is a more practical fading environment, it is useful to determine the performance of STTCs on Nakagami fading channels and evaluate how codes designed for Rayleigh fading perform on these channels. In this thesis we examine the performance of STTCs proposed by Chen et al. [21] over both independent and correlated Nakagami fading channels. We compare our results with the performance of the STTC proposed by Tarokh et al. [5] over independent and correlated Nakagami fading channels [3].

1.5 Outline

Chapter 1 presented a general introduction to the thesis topic, including a brief review of the challenges, solutions and most recent research in STTC. Also we discussed the significance of the research. In Chapter 2 details on STTC and its performance over different channels will be presented. The code performance criteria and construction of STTCs will be discussed. This encoder and decoder structure of STTC based systems will also be presented. Chapter 3 presents simulation results and discusses these results. Performance results for STTCs in Rayleigh and Ricean fading channels as well as for STTCs over both independent and correlated Nakagami fading channels is given. Chapter 4 gives conclusion about our

simulation results and also discusses possible extensions of this research. In particular, implementing iterative decoding for STTC based systems can provide great improvement.

Chapter 2
Space-Time Trellis Code

Introduction

Space-time trellis codes (STTCs) provide both diversity gain and coding gain. In this chapter a brief description of a STTC based wireless system is given in Section 2.1. Then in Section 2.2 we discuss STTC construction. We give a simple example to illustrate this construction. In Section 2.3 we provide a discussion of the performance criteria. We present a rationale for STTC performance over Rayleigh, Ricean and Nakagami fading channels. For each of the different fading channels we explain the different performance criterion. In section 2.4 we present some STTC codes given in the literature. A brief description of channel estimation and STTC decoding is presented in Sections 2.5 and 2.6, respectively. We gave a summary of this chapter in Section 2.7.

2.1 System Model of STTC Based Wireless System

A typical STTC based wireless system has an encoder, pulse shaper, modulator and multiple transmit antennas at the transmitter, and the receiver has one or more receive antennas, demodulator, channel estimator and STTC decoder. We consider a mobile communication system with n_T transmit antennas and n_R receive antennas as shown in Figures 2-1 (a) and (b). The space-time trellis encoder encodes the data $s(t)$ coming from the information source and the encoded data is divided into n_T streams of data $c_t^1, c_t^2, \ldots c_t^{n_T}$. Each of these streams of data passes through a pulse shaper before being modulated. The output of modulator i at time slot t is the signal c_t^i, which transmitted through is transmit antenna i. Here $1 \le i \le n_T$. The transmitted symbols have energy E_s. We assume that the n_T signals are transmitted simultaneously from the antennas. The signals have transmission period T. In the receiver, each antenna receives a superposition of n_T transmitted signals corrupted by noise and multipath fading. Let the complex channel coefficient between transmit antenna i and receive antenna j have a value of $h_{i,j}(t)$ at time t, where $1 \le j \le n_R$.

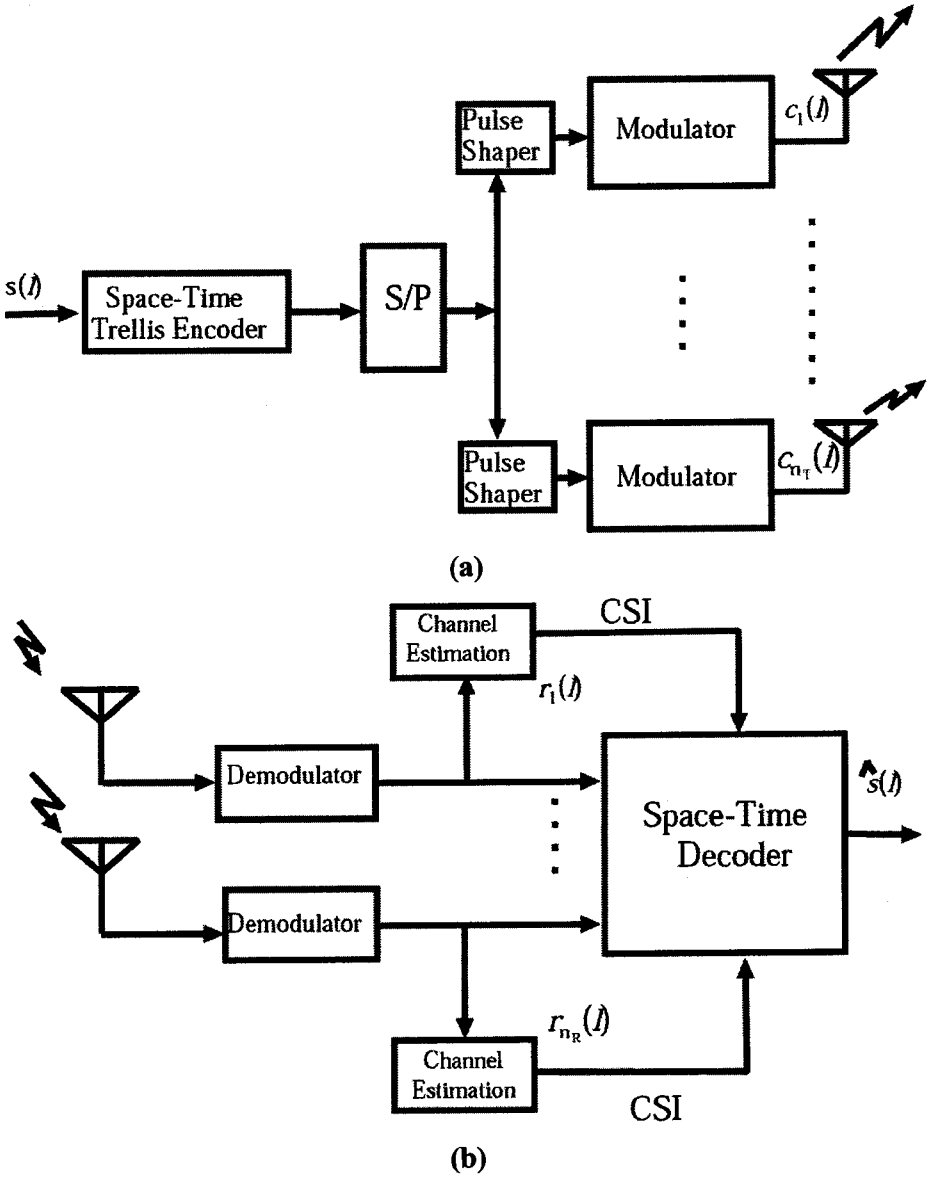

Figure 2.1 A block diagram of the (a) transmitter and (b) receiver of a STTC based system.

The received signal at antenna j, $j = 1, 2, ..., n_R$ [1] is then

$$r_t^j = \sqrt{E_s} \sum_{i=1}^{n} h_{i,j}(t) c_t^i(t) + \eta_t^j , \tag{2.1}$$

where η_t^j is additive white Gaussian noise (AWGN) at receive antenna j, which has zero mean and power spectral density N_0 and $h_{i,j}(t)$ is the channel coefficient between transmit and receive antennas [22].

2.2 Code Construction

STTCs are represented in a number of ways, such as the trellis form or generator matrix form as illustrated in Figure 2.2 for a simple STTC. In [9], most codes are presented in trellis form. But for a systematic code search, the generator matrix form is preferable. The generator matrix representation is also used for convolutional codes [27], [28] and [29]. However the generator matrix notation as shown in Figure 2.2 (b) is a little different than that used for convolutional codes [16]. In Figure 2.2(b) two input bits enter the encoder every symbol period. The input streams are multiplied by the branch coefficients, which can be put into a matrix form (generator matrix) as shown below

$$G = \begin{bmatrix} a_0^1 & b_0^1 & a_1^1 & b_1^1 \\ a_0^2 & b_0^2 & a_1^2 & b_1^2 \end{bmatrix}$$

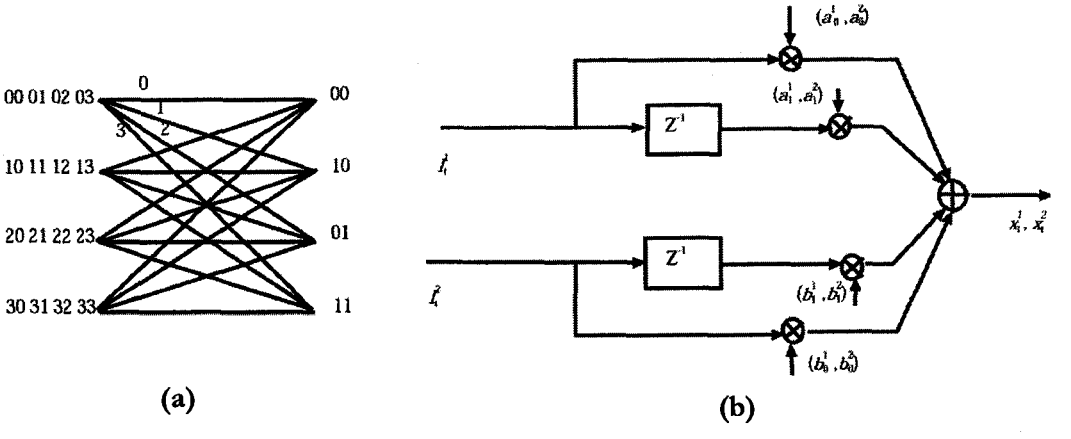

Figure 2.2 (a) Trellis diagram and (b) generator matrix description of a STTC.

The following example illustrates STTC encoding. In Figure 2.3 we provide a trellis diagram and a table of output symbols related to the input bits and current state. This trellis is for 4-PSK constellations. Let the input symbol stream to the encoder is [2 3 2 1 0 1....]. Initially the encoder is in state "0". Thus "0" will be transmitted from the first antenna, the second

antenna transmits "2" and the encoder goes into state "2" [15]. In this way for this input symbol stream the output for the 4-PSK STTC is as follows

$$c = \begin{bmatrix} 0 & 2 & 3 & 1 & 0 & 1 \\ 2 & 3 & 1 & 0 & 1 & .... \end{bmatrix}.$$

State	Output Symbols			
	Input 0	Input 1	Input 2	Input 3
0	00	01	02	03
1	10	11	12	13
2	20	21	22	23
3	30	31	32	33

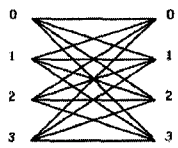

Figure 2.3 4-PSK 4-state STTC

2.2.1 Code Construction of 4-state 4-PSK STTC

A signal constellation diagram for 4-PSK is shown in Figure 2.4. With PSK information is contained in the signal phase. For 4-PSK, the phase takes one of four equally spaced values, such as 0, $2\pi/4$, $4\pi/4$ and $6\pi/4$. These are typically represented by a Gray code [30] and [27], as shown on the right side of Figure 2.4. These signal points are also labeled as 0,1,2 and 3. We can also express these in complex notation.

The encoder structure of a 4-state 4-PSK STTC is shown in Figure 2.5 (b), with bits input to the upper and lower branches. The memory order of the upper and lower branches are υ_1 and υ_2, respectively. These are basically shift registers. The main purpose of the shift registers in the encoder is to store the previous transmitted bits. The length of the shift register is the memory of the encoder. The branch coefficients are arranged alternatively in the generator matrix, with a_i representing the most significant bit (MSB). The input bit streams I_t^1 and I_t^2 are fed into the branches of the encoder with I_t^1 being the MSB. The output of the encoder is [19] [5]

$$x_t^k = \left(\sum_{p=0}^{v1} I_{t-p}^1 . a_p^k + \sum_{q=0}^{v2} I_{t-q}^2 . b_{t-q}^k \right) \qquad \text{mod } 4 \quad k = 1,2,$$

where $\upsilon_1 + \upsilon_2 = \upsilon$ and the number of states is 2^{υ} . υ_i is calculated as

$$\upsilon_1 = \left\lfloor \frac{(\upsilon + i - 1)}{2} \right\rfloor, \quad i = 1,2$$

Here $\lfloor x \rfloor$ denotes the largest integer smaller than or equal to x. For each branch, the output is the sum of the current input scaled by a coefficient and the previous input scaled by another coefficient. The two streams of input bits are passed through their respective shift register branches and multiplied by the coefficient pairs (a_p^1, a_p^2) and (b_q^1, b_q^2) . Here $a_p^k, b_q^k \in \{0,1,2,3\}, k = 1,2, p = 0,1,\ldots,\upsilon_1, q = 0,1,\ldots,\upsilon_2$.

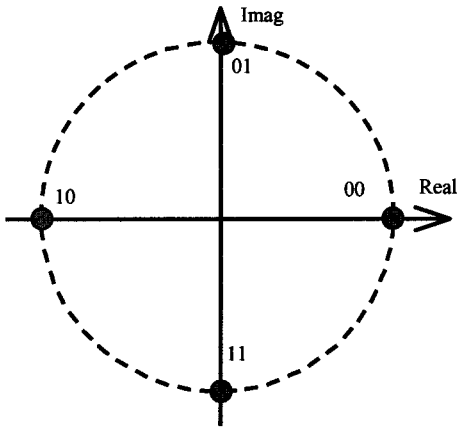

$0 \rightarrow 00 \Leftrightarrow 1 + 0j$
$1 \rightarrow 01 \Leftrightarrow 0 + 1j$
$2 \rightarrow 10 \Leftrightarrow -1 + 0j$
$3 \rightarrow 11 \Leftrightarrow 0 - 1j$

Figure 2.4 4-PSK signal constellation diagram

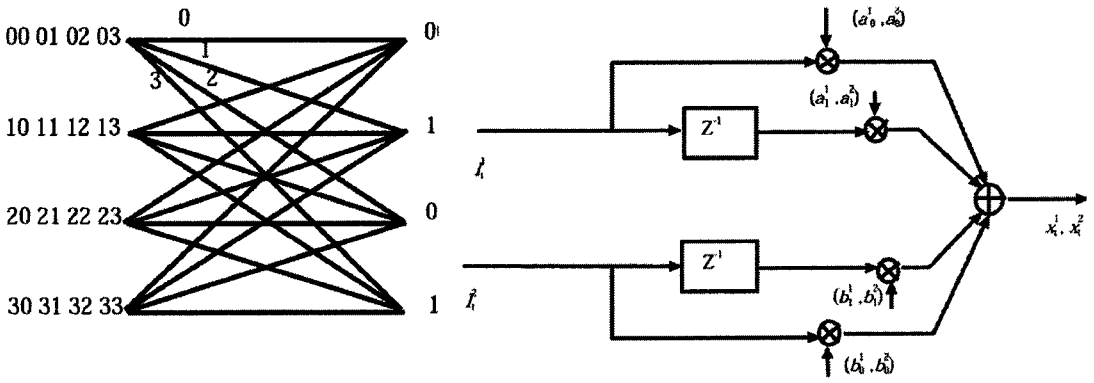

(a) (b)

Figure 2.5 4 PSK 4-state STTC (a) Trellis diagram (b) Encoder Structure

Then x_t^1 and x_t^2 are transmitted simultaneous through the first and second transmit antennas, respectively. Figures 2.6 (a) and (b) shows 8-state and 16 -state trellis diagrams respectively, for a rate of 2 b/s/Hz [9].

2.2.2 Code Construction of 8-state 8 PSK STTC

The 8 PSK, 8-state signal state constellation is shown in Figures 2.7. The trellis diagram and encoder structure of the 8-state 8 PSK trellis code is shown in Figure 2.8. This is similar to that shown in Figure 2.5 except that it has three input (transmit) antennas and three sets of coefficients. The additional input I_t^3 corresponds to a branch of memory order υ_3. The total memory order is $\upsilon = \upsilon_1 + \upsilon_2 + \upsilon_3$. Here

$$\upsilon_i = \left\lfloor \frac{\upsilon + i - 1}{3} \right\rfloor \qquad i = 1,2,3$$

The coefficient pairs are $(a_p^1, a_p^2), (b_q^1, b_q^2)$ and (c_s^1, c_s^2) for the input streams I_t^1, I_t^2 and I_t^3 respectively. The encoder output is

$$x_t^k = \left(\sum_{p=0}^{v} I_{t-p}^1 . a_p^k + \sum_{q=0}^{v_2} I_{t-q}^2 . b_{t-q}^k + \sum_{s=0}^{v_3} I_{t-s}^3 . b_{t-s}^k \right) \quad \text{mod } 8 \text{ and } k = 1,2$$

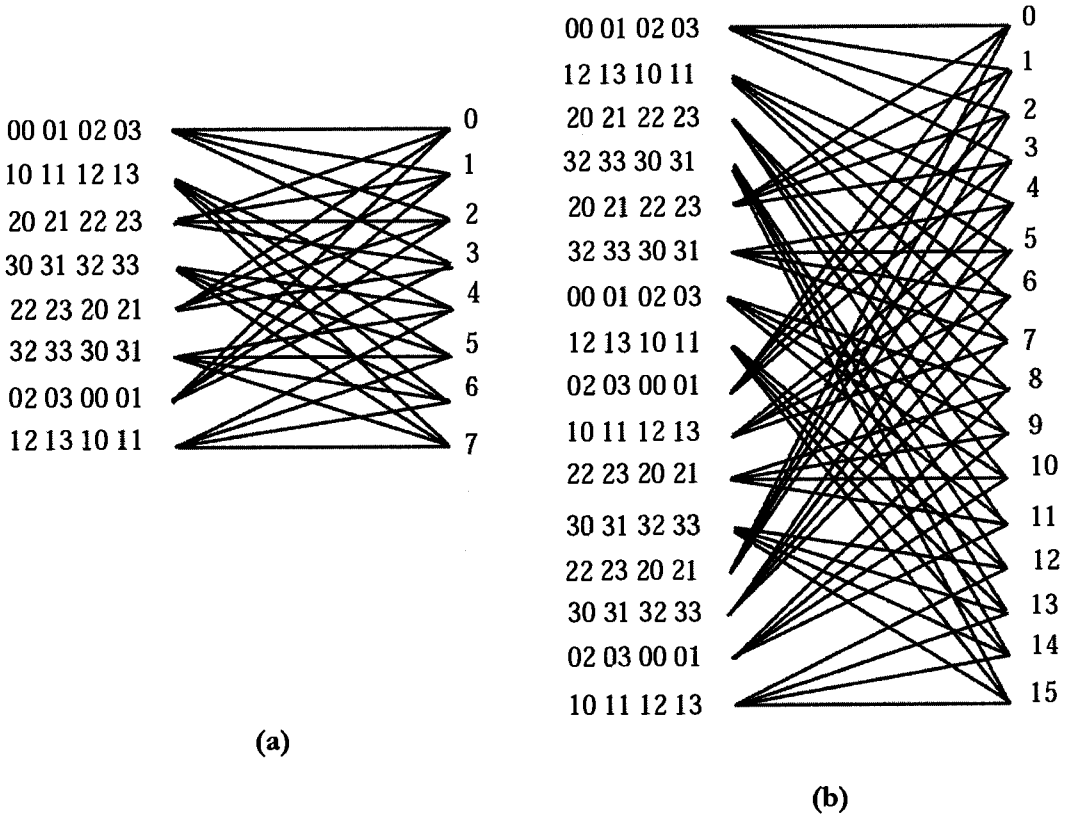

Figure 2.6 (a) Trellis diagram of 4 PSK 8-state STTC

(b) Trellis diagram of 4 PSK 16-state STTC

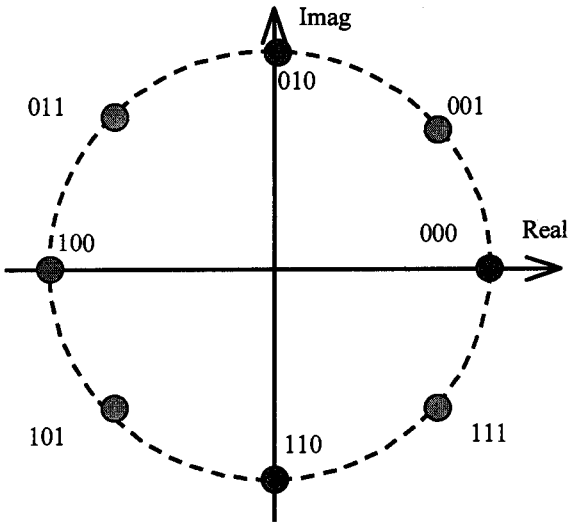

$$0 \rightarrow 000 \Leftrightarrow 1+0j$$

$$1 \rightarrow 001 \Leftrightarrow \frac{\sqrt{2}}{2}+\frac{\sqrt{2}}{2}j$$

$$2 \rightarrow 010 \Leftrightarrow 0+1j$$

$$3 \rightarrow 011 \Leftrightarrow -\frac{\sqrt{2}}{2}+\frac{\sqrt{2}}{2}j$$

$$4 \rightarrow 100 \Leftrightarrow -1+0j$$

$$5 \rightarrow 101 \Leftrightarrow -\frac{\sqrt{2}}{2}-\frac{\sqrt{2}}{2}j$$

$$6 \rightarrow 110 \Leftrightarrow 0-1j$$

$$7 \rightarrow 111 \Leftrightarrow \frac{\sqrt{2}}{2}-\frac{\sqrt{2}}{2}j$$

Figure 2.7 8-PSK Signal constellation

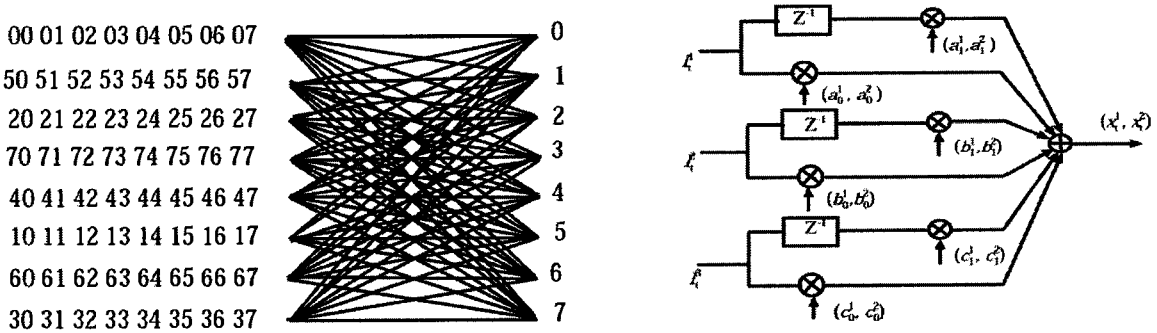

(a) **(b)**

Figure 2.8 (a) Trellis diagram and (b) encoder structure of an 8-PSK 8-state STTC

2.3 Performance Criteria

We assume that the STTC codeword is given by

$$c = (c_1^1 c_1^2 ... c_1^{n_T} c_2^1 c_2^2 ... c_2^{n_T} ..... c_l^1 c_l^2 .... c_l^{n_T}),$$

where l is the frame length. We consider a maximum likelihood receiver, which may possibly decide on an erroneous code word e, given by

$$e = (e_1^1 e_1^2 ... e_1^{n_T} e_2^1 e_2^2 ... e_2^{n_T} ..... e_l^1 e_l^2 .... e_l^{n_T})$$

We can write the difference code matrix, the difference between the erroneous codeword and the transmitted codeword as follows -

$$B(c,e) = \begin{pmatrix} e_1^1 - c_1^1 & e_2^1 - c_2^1 & \dots & \dots & e_l^1 - c_l^1 \\ e_1^2 - c_1^2 & e_2^2 - c_2^2 & \dots & \dots & e_l^2 - c_l^2 \\ e_1^3 - c_1^3 & e_2^3 - c_2^3 & \ddots & \vdots & e_l^3 - c_l^3 \\ \vdots & \vdots & \ddots & \ddots & \vdots \\ e_1^{n_T} - c_1^{n_T} & e_2^{n_T} - c_2^{n_T} & \dots & \dots & e_l^{n_T} - c_l^{n_T} \end{pmatrix}. \quad (2.2)$$

The difference matrix $B(c,e)$ has dimension $n_T \times l$. From [9] we know that to achieve the maximum diversity order $n_R.n_T$ (n_R receive antennas, n_T transmit antennas) matrix $B(c,e)$ must have full rank for all possible codewords c and e. If $B(c,e)$ has minimum rank r over the set of pairs of distinct codewords then the diversity will be $r.n_R$ [9].

Let $A(c,e) = B(c,e)B^*(c,e)$ be the distance matrix, where $B^*(c,e)$ is the Hermitian of $B(c,e)$. The rank of $A(c,e)$ is r. A has minimum dimension $n_T - r$ and exactly $n_T - r$ eigenvalues of A are zero. The non-zero eigenvalues of A are denoted by $\lambda_1, \lambda_2, \lambda_3, ... \lambda_n$. Assuming perfect channel state information (CSI), the probability of transmitting c and deciding on an erroneous codeword e at the decoder is given by [5] [9] [19]

$$P(c,e \mid h_{i,j}, i = 1,2,\dots,n_T, j = 1,2,\dots,n_R) = Q\left(\sqrt{\frac{E_s}{2N_0} d^2(c,e)}\right),$$

or,

$$P(c \to e \mid h_{i,j}, i = 1,2,\dots,n_T, j = 1,2,\dots,n_R) \le \exp(-d^2(c,e)E_s / 4N_0), \quad (2.3)$$

where $N_0/2$ is the noise variance per dimension and

$$d^2(c,e)=\sum_{j=1}^{n_R}\sum_{t=1}^{l}\left|\sum_{i=1}^{n_T}h_{i,j}(c_t^i-e_t^i)\right|^2$$

is the Euclidean distance. For independent Ricean fading we can (2.4) as [5]

$$P(c\to e)\le\prod_{j=1}^{n_R}\left(\prod_{i=1}^{n_T}\frac{1}{1+\frac{E_s}{4N_0}\lambda_i}\exp\left(-\frac{K_{i,j}\frac{E_s}{4N_0}\lambda_i}{1+\frac{E_s}{4N_0}\lambda_i}\right)\right). \tag{2.4}$$

Here $K_{i,j}$ is a coefficient and it is described in details in [5].

For the special case of Rayleigh fading we can assume $K_{i,j}$ =0 for all i and j [5]. Then (2.4) can be written as

$$P(c\to e)\le\left(\frac{1}{\prod_{i=1}^{n_T}\left(1+\frac{E_s}{4N_0}\lambda_i\right)}\right)^{n_R} \tag{2.5}$$

Let r denote the rank of matrix $A(c,e)$. The matrix A has dimension n_T-r and n_T-r eigenvalues of A are zero.

$$P(c\to e)\le\left(\prod_{i=1}^{r}\lambda_i\right)^{-n_R}\left(\frac{E_s}{4N_0}\right)^{-rn_R} \tag{2.6}$$

We can derive following Design criteria for the STTC to achieve the best performance of a given system [5].

2.3.1 Design Criteria for STTC over Rayleigh Fading

2.3.1.1 Rank Criterion

The rank criterion optimizes the spatial diversity gain achieved by a STTC. Assume $B(c,e)$ has minimum rank r over the set of pairs of distinct codewords so a diversity of $r.n_R$ is achieved [5][19]. To illustrate this criterion [31], consider a 4-PSK system where the transmitted codeword is $c=220313$, and the erroneous codeword the receiver decides upon

is $e = 330122$. Figure 2.4 gives the 4-PSK signal constellation. In this example, $n_T = 2$ and the message length is $L = 3$. The 2 x 3 difference matrix is

$$B(c,e) = \begin{vmatrix} -j-(-1) & 1-1 & -1-j \\ -j-(-1) & j-(-j) & -1-(-j) \end{vmatrix}$$

$$= \begin{vmatrix} 1-j & 0 & -1-j \\ 1-j & 2j & j-1 \end{vmatrix}.$$

The rank of $B(c,e)$ is 2, as is the rank of $A(c,e)$. For this system with $n_T = 2$ transmit antennas and $n_R = 1$ receive antenna, the diversity gain is 2.

2.3.1.2 Determinant Criterion

The determinant criterion optimizes the coding gain. Recall that r is the rank of $A(c,e)$. Coding gain corresponds to the minimum r th roots of the sum of the determinants of all $r \times r$ principal cofactors of $A(c,e) = B(c,e)B^*(c,e)$ taken over all pairs of distinct codewords c and e [5]. Now $(\lambda_1 \lambda_2 \ldots \lambda_r)$ is the absolute value of the sum of the determinants of all principal $r \times r$ cofactors of A. Thus if a diversity advantage of $n_R r$ is achieved, the coding gain is $(\lambda_1 \lambda_2 \ldots \lambda_r)^{1/r}$. So if maximum diversity of $n_R n_T$ is the design target then we have to maximize the minimum determinant of $A(c,e)$. From the example, for the rank criterion the eigenvalues of the matrix A are

$$\lambda_1 = -2.2679 - 3j$$
$$\lambda_2 = -5.7321 - 3j$$

For $r = 2$, the coding gain for the codeword given in the example is 4.9327 [31].

2.3.1.3 Euclidean distance Criterion

When the diversity gain is large (with two or more receive antennas), [21] proposes another design criteria, namely the Euclidean Distance Criteria (EDC). According to [21], the Rank and Determinant criteria (RDC) applies to the systems with a single receive antenna and a

small number of transmit antennas. This shows that with diversity gain $rn_R \geq 4$, [12] shows that the error probability is upperbounded by

$$P_e(c \to e) \leq \frac{1}{4}\exp\left(-n_R \frac{E_s}{4N_0}\sum_{i=1}^{n_T}\sum_{j=1}^{l}|e_j^i - c_j^i|\right)$$
$$when \qquad (2.7)$$
$$rn_R \geq 4$$

which indicates that we should maximize the minimum squared Euclidean distance between any two different codewords [21].

2.3.2 Design Criteria for STTC over Ricean Fading

Equation (2.4) gives the probability of error for independent Ricean distributions. If we consider (2.4) for sufficiently high signal-to-noise ratios, we get [5]

$$P(c \to e) \leq \left(\frac{E_s}{4N_0}\right)^{-rn_R}\left(\prod_{i=1}^{r}\lambda_i\right)^{-n_R}\left[\prod_{j=1}^{n_R}\prod_{i=1}^{r}\exp\left(-K_{i,j}\right)\right] \qquad (2.8)$$

Thus we get a diversity gain of $r.n_R$ and a coding gain of

$$\left(\lambda_1\lambda_2\ldots\lambda_r\right)^{1/r}\left[\prod_{j=1}^{n_R}\prod_{i=1}^{r}\exp(-K_{i,j})\right]^{1/rn_R}$$

2.3.2.1 Rank Criterion

The rank criterion is the same as for the Rayleigh channel [5].

2.3.2.2 Determinant Criterion

We assume $\Lambda(c,e)$ denotes the sum of all determinants of the $r \times r$ principal cofactors of the matrix $A(c,e)$. Here r is the rank of $A(c,e)$. To achieve the maximum coding gain the minimum of the products

$$\Lambda(c,e)^{1/r}[\prod_{j=1}^{n_R}\prod_{i=1}^{r}\exp(-K_{i,j})]^{1/rn_R}$$

taken over all pairs of codewords c and e has to be maximized.

2.3.3 STTC over Nakagami Fading Channels

In the multipath fading channel model literature, the Rayleigh and Ricean distributions are frequently used. However, the Nakagami model is often more versatile than the above-mentioned channels [3]. In this model it is assumed that the received signal is the sum of vectors with random amplitudes and random phases. This assumption makes this model more flexible than the Rayleigh and Ricean distributions [2]. The Nakagami distribution is given by

$$p(\alpha) = \frac{2}{\Gamma(m)}\left(\frac{m}{\Omega}\right)^m \alpha^{2m-1} e^{-\alpha^2 m/\Omega} \quad , \tag{2.9}$$

where $\Gamma(x)$ denotes the Gamma function of x, and

$$\Omega = E[\alpha^2],$$

$$m = \frac{\Omega^2}{E[(\alpha^2 - \Omega)^2]}, m \geq 1/2.$$

The notation $E[x]$ denotes the expected value of x. The constant m is called the inverse fading parameter, with $m = 1$ and $m = \infty$ corresponding to Rayleigh fading and no fading, respectively.

2.3.3.1 Independent Fading

The amplitudes of $h_{i,j}$ are identical and independent m-distributed with the same m and Ω. Pairwise error probability is given by [3],

$$P(c \to e) \leq \frac{(m/\Omega)^m}{\Gamma(m)} \prod_{j=1}^{m} \prod_{i=1}^{n} \frac{\Gamma(m)}{\left(\frac{E_s}{4N_0}\lambda_i + \frac{m}{\Omega}\right)^m}. \tag{2.10}$$

Here $\Gamma(m)$ is gamma function which means $\Gamma(n) = \int_0^\infty t^{n-1} e^{-t} dt$, $n > 0$. Equation

$$P(c \to e)$$

$$\leq f(m)\left(\prod_{i=1}^{r}\left(\lambda_i + \frac{4N_0 m}{E_s \Omega}\right)\right)^{-mn_R}\left(\frac{E_s}{4N_0}\right)^{-rmn_R}$$

$$\leq f(m)\left(\prod_{i=1}^{r}(\lambda_i)\right)^{-mn_R}\left(\frac{E_s}{4N_0}\right)^{-rmn_R} . \qquad (2.11)$$

Here $f(m)=(m/\Omega)^{m-mn_R(n_T-r)}\Gamma(m)^{n_Tn_R-1}$ [3].

From (2.11), the diversity order is rmn_R. This is in fact m times the diversity order that can be achieved in Rayleigh fading. The coding gain is $f(m)=(m/\Omega)^{-1/rmn_R}\left(\prod_{i=1}^{r}\lambda_i\right)^{1/r}$ [22]. Now for $m=1,\Omega=1$ we can simplify (2.14) as [3]

$$P(c\rightarrow e)\leq\left(\prod_{i=1}^{r}(\lambda_i)\right)^{-n_R}\left(\frac{E_s}{4N_0}\right)^{-rn_R} \qquad (2.12)$$

This agrees with (2.6) which is the error probability for Rayleigh fading. If we compare (2.11) and (2.12) we see that the only difference between them is the factor $f(m)$ and m on the right hand side of (2.14). Thus we can say that the diversity order achieved in Rayleigh fading increases by a factor of m in Nakagami fading and the coding gain is multiplied by a factor of $f(m)^{-1/rmn_R}$. We can consider this factor as the additional coding gain due to Nakagami fading [3].

2.3.3.2 Correlated Fading

In this section we present the design criteria for STTC in correlated fading. We considered the case when the fading coefficients, $h_{i,j}$ are correlated. We assume that the envelopes of $h_{i,j}$ are modeled as identically correlated Nakagami distributed random variables [3]. In [3] it is shown that rank and determinant criteria is similar to the independent Nakagami fading criteria. We presented simulation results of performance of the STTC over correlated Nakagami fading in Section 3.4.2.

2.4 Code Search with the Performance Criteria

The RDC and EDC are usually used to guide the computer search for good space-time trellis codes. Many search results are given in [16], [19], [20], [18], [21] and [22]. Some of these are

simulated in this thesis. Because of the computational complexity of the pair-wise error probability bound equations, computer simulation is usually carried out to more accurately evaluate the code performance. No comparison results between the upper bound and the simulation results have been given in the literature to date. Performance criteria in the presence of channel estimation errors and multipath effects are discussed in [11]. It was shown that the design criteria also apply to Nakagami fading channels in [3]. The performance criteria and simulation results for space-time trellis codes over frequency selective fading channels was presented in [3].

In the following tables we present the codes designed by Tarokh et al. in [5], [9] and the codes designed by Chen et al. in [19] and [21]. These tables also give the number of states $\left(2^{\upsilon}\right)$, the minimum rank $\left(r\right)$ the minimum determinant $\left(\det\right)$ and the minimum squared Euclidean distance $\left(d^2_{\min}\right)$. Tables 1 and 3 presents the 4,8,16 and 32-state 4 PSK and 8 PSK STTC codes proposed by Tarokh et al. [5] [9] for a system with two transmit antennas. These codes were designed using the rank and determinant criteria (RDC). From the tables we can see these codes have full rank $r = n_T$ and maximum minimum determinant of the code distance matrices $A(c,e)$. Tables 2 and 4 present the 4,8,16 and 32-state 4 PSK and 8 PSK STTC codes proposed by Chen et al. [19] [21] for a system with two transmit antennas. These codes were designed using the Euclidean distance criteria (EDC). The code design using RDC for wireless systems with transmit antennas $n_T \geq 3$ is quite complex [21], so for this case the Euclidean distance criteria (EDC) was used in [21] to design codes. Tables 5 and 6 present the 4,8,16 and 32-state 4 PSK STTC codes proposed by Chen et al. [21] for systems with 3 and 4 transmit antennas, respectively. From these tables it is evident that the codes based on the EDC have the same same value for r, but they have a larger Euclidean distance $\left(d^2_{\min}\right)$ compared with the codes designed based on the RDC.

TABLE 1

4-PSK Trellis codes for two transmit antennas proposed by Tarokh et al. [5]

2^{υ}	a_0^1, a_0^2	a_1^1, a_1^2	a_3^1, a_3^2	a_3^1, a_3^2	b_0^1, b_0^2	b_1^1, b_1^2	b_2^1, b_2^2	b_3^1, b_3^2	r	det	d^2_{min}
4	(0,2)	(2,0)	--	--	(0,1)	(1,0)	--	--	2	4	4
8	(0,2)	(2,0)	--	--	(0,1)	(1,0)	(2,2)	--	2	12	8
16	(0,2)	(2,0)	(0,2)	--	(0,1)	(1,2)	(2,0)	--	2	12	8
32	(0,2)	(2,0)	(3,3)	--	(0,1)	(1,1)	(2,0)	(2,2)	2	12	12

TABLE 2

4-PSK Trellis codes for two transmit antennas proposed by Chen et al. [19]

2^{υ}	a_0^1, a_0^2	a_1^1, a_1^2	a_3^1, a_3^2	a_3^1, a_3^2	b_0^1, b_0^2	b_1^1, b_1^2	b_2^1, b_2^2	b_3^1, b_3^2	r	det	d^2_{min}
4	(0,2)	(1,2)	--	--	(2,3)	(2,0)	--	--	2	4	10
8	(2,2)	(2,1)	--	--	(2,0)	(1,2)	(0,2)	--	2	8	12
16	(1,2)	(1,3)	(3,2)	--	(2,0)	(2,2)	(2,0)	--	2	8	16
32	(0,2)	(2,3)	(1,2)	(3,2)	(2,2)	(1,2)	(2,3)	(2,0)	2	20	16

TABLE 3

8-PSK Trellis codes for two transmit antennas proposed by Tarokh et al. [5]

2^{υ}	a_0^1, a_0^2	a_1^1, a_1^2	b_0^1, b_0^2	b_1^1, b_1^2	b_2^1, b_2^2	c_0^1, c_0^2	c_1^1, c_1^2	c_2^1, c_2^2	r	det	d^2_{min}
8	(0,4)	(4,0)	(0,2)	(2,0)	--	(0,1)	(5,0)	--	2	2	4
16	(0,4)	(4,4)	(0,2)	(2,2)	--	(0,1)	(5,1)	(1,5)	2	3.515	6
32	(0,4)	(4,4)	(0,2)	(2,2)	(2,2)	(0,1)	(5,1)	(3,7)	2	3.515	8

TABLE 4

8-PSK Trellis codes for two transmit antennas proposed by Chen et al. [19]

2^{υ}	a_0^1, a_0^2	a_1^1,a_1^2	b_0^1,b_0^2	b_1^1, b_1^2	b_2^1,b_2^2	c_0^1, c_0^2	c_1^1, c_1^2	c_2^1, c_2^2	r	det	d^2_{min}
8	(2,1)	(3,4)	(4,6)	(2,0)	--	(0,4)	(4,0)	--	2	2	7.172
16	(2,4)	(3,7)	(4,0)	(6,6)	--	(7,2)	(0,7)	(4,4)	2	0.686	8
32	(0,4)	(4,4)	(0,2)	(2,3)	(2,2)	(3,0)	(2,2)	(3,7)	2	2.343	8.586

TABLE 5

4-PSK Trellis codes for three transmit antennas proposed by Chen et al. [21]

2^{υ}	a_0^1,a_0^2, a_0^3	a_1^1,a_1^2, a_1^3	b_0^1,b_0^2, b_0^2	b_1^1,b_1^2, b_1^2	c_0^1,c_0^2, c_0^3	c_1^1,c_1^2, c_1^3	c_2^1,c_2^2, c_2^3	r	det	d^2_{min}
4	(0,2,2)	--	(2,3,3)	--	(1,2,3)	(2,0,2)	--	2	0	16
8	(2,2,2)	--	(2,0,3)	(1,2,0)	(2,1,1)	(0,2,2)	--	2	0	20
16	(1,2,1)	(2,2,0)	(2,0,2)	(3,2,1)	(1,3,2)	(2,0,2)	--	2	0	24
32	(0,2,2)	(1,2,2)	(2,2,0)	(1,2,2)	(2,3,3)	(2,3,1)	(2,0,0)	2	0	24

TABLE 6

4-PSK Trellis codes for four transmit antennas proposed by Chen et al. [21]

2^{υ}	a_0^1,a_0^2, a_0^3, a_0^4	a_1^1,a_1^2, a_1^3, a_1^4	b_0^1,b_0^2, b_0^2, b_0^4	b_1^1,b_1^2, b_1^2, b_1^4	c_0^1,c_0^2, c_0^3, c_0^4	c_1^1,c_1^2, c_1^3,c_1^4	c_2^1,c_2^2, c_2^3, c_2^4	r	det	d^2_{min}
4	(0,2,2,0)	--	(2,3,3,2)	--	(1,2,3,2)	(2,0,2,1)	--	2	0	20
8	(2,2,2,2)	--	(2,0,3,1)	(1,2,0,3)	(2,1,1,2)	(0,2,2,1)	--	2	0	26
16	(1,2,1,1)	(2,2,0,0)	(2,0,2,2)	(3,2,1,2)	(1,3,2,2)	(2,0,2,2)	--	$\leq$ 3	0	32
32	(0,2,2,2)	(1,2,2,0)	(2,2,0,1)	(1,2,2,1)	(2,3,3,2)	(2,3,1,0)	(2,0,0,2)	$\leq$ 3	0	36

2.5 STTC Decoder

The decoder is based on the Viterbi algorithm, so it uses the trellis structure of the code. Each time the decoder receives a pair of channel symbols it computes a metric to measure

the "distance" between what is received and all of the possible channel symbol pairs that could have been transmitted. For hard decision Viterbi decoding the Hamming distance is used, and the Euclidean distance is used for soft decision Viterbi decoding. The metric values computed for the paths between the states at the previous time instant and the states at the current time instant are called "branch metrics". We assume that the decoder has ideal channel state information (CSI) and thus knows the path gains $h_{i,j}$ (where $i = 1, 2, \ldots, n_T$ and $j = 1, 2, \ldots, n_R$). If the signal is r_t^j at receive antenna j and time t, the branch metric for a transition labeled $x_t^1 x_t^2 \ldots x_t^{n_T}$ is given by [1]

$$\sum_{j=1}^{n_R} \left| r_t^j - \sum_{i=1}^{n_T} h_{i,j} q_t^i \right|^2$$

The Viterbi algorithm determines the path with the lowest accumulated metric.

2.6 Summary of Space-Time Coding

Section 2.1 of this chapter gave a brief description of a STTC based wireless system. We showed and explained the transmitter and receiver of such system. Section 2.2 gave an explanation of the construction of a STTC. In the beginning of this section we gave a simple example of how information is coded in STTC based systems. Later we discussed code construction and the encoder structure of 4-state 4-PSK and 8-state 8-PSK STTC. In Section 2.3 we discussed about different performance criterion. We presented a details of the RDC and EDC, and provided design criteria over Rayleigh, Ricean and Nakagami fading. In Section 2.4 we presented the codes designed by Tarokh et al. and Chen et al. in six tables. Section 2.5 briefly discussed STTC decoders.

The design criteria for code construction of space-time trellis codes assume that perfect channel state information (CSI) is available at the receiver, i.e., the receiver knows the exact channel path gains. In reality, it is impossible for the receiver to have perfect channel information, however the receiver can estimate CSI. Due to estimation errors performance degradation will occur. Several techniques have been introduced to estimate the channel [32], [33] and [34]-[37].

CHAPTER 3
SIMULATION AND RESULTS

Introduction

In Chapter 2 we discussed space-time codes and the design criteria proposed by Tarokh et al. [5] and Chen et al. [19] [21]. The codes proposed in [16] by Baro et al. showed significant improvement performance over the codes in [5], but the codes designed in [19] and [21] showed better performance than those in [16]. This is the reason we choose the codes in [19] and [21] (given in Tables 2, 4, 5 and 6), over the codes designed in [16]. This chapter presents the performance of the STTCs given in [5], [19] and [21] over different fading channels. The code performance is evaluated by simulation over Rayleigh, Nakagami and Ricean fading channels.

3.1 Simulation Parameters

In our simulations we considered the IS-136 standard [3]. In this system, performance is measured by the frame error rate (FER) for a frame consisting of 130 symbols. We also assumed ideal channel state information (CSI) is available at the receiver. We carried out the simulation by MATLAB. Random M-PSK symbols are set in frames as a group, which consists of 130 symbols each. The space-time encoder takes the frame as input and generates codeword pairs of each input symbol simultaneously for all the transmit antennas. Pulse shaping and matched filter are used. These complex signals are transmitted through the MIMO channel. We modeled the signals and channels in base-band. So modulation/demodulation operations are not carried out. We used Monte Carlo simulation to carry out the FER evaluation of the space-time coded system. The FER is given by

$$p_e = \lim_{F \to \infty} \frac{F_e}{F}$$

where F is the total number of transmitted frames and F_e is the total number of erroneous frames received at the receiver. It is impossible to run the simulation for an infinite length of

time, so we take F as a very large number. The maximum number of iterations used was 50,000 for a FER above 10^{-3}.

3.2 STTC performance over Rayleigh Channels

In Figures 3.1 and 3.2 we show the performance in independent flat Rayleigh fading channels of the 4/8/16/32-states codes with two transmit antennas and 1/2/4 receive antennas for 4/8-PSK constellations. These codes were proposed by Tarokh et al. [5] and were designed with the rank and determinant criteria in a heuristic manner [5]. We presented these codes in Table 1 of Chapter 2.

It is seen in Figure 3.1 that the performance improves as the number of states increases. We can also see that the coding gain between the 4-state and 8-state codes is larger than the others. When we use multiple receiver antennas a significant improvement is achieved for all of the codes. This improvement is due to diversity gain. Bandwidth efficiency of the 4-PSK codes is 2 bits/s/Hz. Figure 3.2 presents the code performance of the 8 and 16-state codes for 8-PSK constellations. It is evident that these also follow the same trend as the 4-PSK codes, but performance of 8-PSK 8-state codes is approximately 4.1 dB worse than the 4-PSK 8-state codes for the case of two receiver antennas (n_R=2) and two transmit antennas (n_T=2). With a system with n_R=4 and n_T=2 we can see from Fig 3.2 the 8-PSK 8-state codes perform approximately 3.75 dB worse than the 4-PSK 8-state codes. The reason for this phenomenon is that for 8-PSK codes the signal points are much closer together.

There are several papers which presented improved codes [16], [17], [19] and [21], but the codes proposed by Chen et al. [19] [20] [21] and [38] showed much better performance than the others. The performance of the codes presented in Table 2 and 4 proposed by Chen et al. [12] and [21] are shown in Figure 3.3. Here we compare the codes from Table 2 with the performance of the codes of Table 1. We found that the 4-state codes of Table 2 outperform the 4-state codes of Table 1 by approximately 1 dB for a system having n_T=2 and n_R=2. We also see that the 8,16 and 32-state codes of Table 2 outperform the codes of Table 1 by almost 1 dB in every case. Figure 3.4 shows the performance over flat Rayleigh fading channels of the 4/8/16/32-state 4-PSK codes presented in Table 5 for a system with three

transmit (n_R=3) antennas and 2/4 receive antennas designed by Chen et al. [21]. We found these codes outperform the codes designed for 2 transmit antennas. For n_R=2 the performance of the 4, 8, 16 and 32-state STTCs in a system with n_T=3 outperform the n_T=2 codes by about 0.25dB, 0.75dB, 1 dB and 1 dB respectively. Figure 3.5 presents the performance of the STTC presented in Table 6 [21] over flat Rayleigh fading channels with n_T=4 antennas and 2/4 receive antennas. Comparing this figure with Figure 3.4, we found that a system with n_T=4, n_R=2 shows 0.75,1.25,1.0 and 1.25 dB improvement for 4,8,16 and 32-states respectively, over the codes from Table 5. From the above simulation results we found that for 3 or 4 transmit antennas we achieved significant performance improvements.

3.2.1 Summary

In the case of Rayleigh Fading channels we see that as we increase the number of states from 4 to 32 the performance of the system improves. Also when we increase the number of receiver antennas n_R we found that system performance improves. This improvement is due to the diversity. Codes from Table 2 outperform the codes from Table 1 in a system with 2 transmit antennas and multiple receive antennas. Codes designed by EDC shows performance improvement when we increase the number of transmit antennas from 2 to 3 and 4. The performance improvement due to increasing number of receive antennas is better than the amount of improvement obtained by employing more transmit antenna because the transmit power is kept constant equally divided amongst the transmit antennas.

3.3 STTC Performance over Ricean Channels

In this section we show the performance of STTCs over Ricean channels. Here K is the Rice factor, which is the specular-to-diffuse ratio of the received signal. As discussed in Chapter 2, Ricean fading models a direct signal path (the specular component) in addition to reflected signals (the diffuse component). The higher the Rice factor, the less severe is the fading. For a specular-to-diffuse ratio <=-6 dB (K=0.25) the fading performance very closely approximates the Rayleigh fading.

Figure 3.6 presents the performance of the 4-PSK 4-state code designed by Tarokh et al. (in Table 1) over Ricean fading channels with different values of K for a system consisting of two transmit antennas (n_T=2) and one receive antenna (n_R=1). Here we can see that with K=0.25 the system performs almost the same as in a Rayleigh fading channel. As the value of K increases performance improves. For simulation in this thesis we chose K=3.

In Figure 3.7 we see that the 8-state code in Table 1 outperforms the 4-state code by 1.8 dB, the 16-state code outperforms the 8-state code by 0.5 dB, and the 32-state code outperforms the 16-state code by 0.25 dB. Comparing Figure 3.8 with Figure 3.7 we see that the 4-state STTC of Table 2 outperforms the 4-state STTC of Table 1 by about 1.5 dB.

3.4 STTC Performance over Nakagami Channels

The performance over independent and correlated Nakagami fading channels of the 4-state 4-PSK and 8 –state 4 PSK codes is given in [3] with two transmit antennas. In this section, we show the performance of the 4/8/16/32 states codes presented in Tables 1-6 of Chapter 2.

Figure 3.9 we show the performance of the 4-state 4 PSK codes presented in Table 1 over a Nakagami channel for m =1,2 and 4 two transmit antennas and one receive antenna. From this figure we see that for m = 1, we get the same result as Rayleigh fading channel. As the Nakagami value parameter increases, the code performance improves.

In Figure 3.10 we show the performance of the 4-state 4-PSK code presented in Table 2 over a Nakagami fading channel with m= 1,2 and 4. For m=1 we obtain the same performance as in a Rayleigh fading channel, which was given in Figure 3.9. In Figure 3.11 we found that for a system with n_T=2 and n_R=1, the 4-state 4 PSK code presented in Table 1 performs better than the code presented in Table 2 for all values of m considered. For m = 2 and 4, the code presented in Table 1 outperforms the code in Table 2 by 0.5 dB and 1.4 dB, respectively. From [21], the codes of Table 1 were designed using the Rank and Determinant Criteria (RDC), and these outperform the codes in Table 2 which were designed using the Euclidean Distance Criteria (EDC) for system with n_R=1. According to [12], when rn_R is sufficiently large (>3) performance of STTCs are dominated by the

minimum Euclidean distance of $A(c,e)$ taken over all pairs of distinct codewords c and e. Here we see for n_T=2 and n_R=1 the product rn_R is not large ($r = n_T$). That's why codes from Table 2, which are designed by EDC is not performing worse than codes from Table1. Figures 3.12 and 3.13 give the performance of the 8-state STTCs presented in Tables 1 and 2, respectively for a system with n_R=1,2 and n_T=2. If we compare the results in these figures, we see that the performance of the 8 state codes in Tables 1 and 2 are approximately the same for m=1 (Rayleigh fading channel) and n_R=1. For m=2 and n_R=2, the STTC of Table 2 showed a 0.2dB gain over the STTCs from Table 1. This shows that the code design criterion presented in [21] for a Rayleigh fading channel is also valid for Nakagami fading channel [3].

3.4.1 Independent Fading

In the remainder of this chapter, the Nakagami fading parameter is set to m=2. The performance of the codes presented in Table 1 over independent Nakagami fading channels was shown in [3].

Figure 3.14 and 3.15 present the performance of the 4 and 16 state and 8 and 32 state STTC codes, respectively, in Table 1. Figures 3.16 and 3.17 present the performance of the 4 and 16 state, and 8 & 32 state STTC codes of Table 2. These figures provide results for 1,2 and 4 receiver antennas and two transmit antennas. These results are identical to those in [3].

In Figure 3.18 we compare the 4 and 16-state STTCs in Tables 1 and 2 for a system with n_T=2 and n_R=1 and 4. We chose a large receive diversity (n_R=4) to see the performance more clearly. In the case of n_R=1 and n_T=2 we see that the 4-state code in Table 1 outperforms the corresponding code in Table 2 by 0.5 dB, whereas the 16-state code in Table 1 outperforms the corresponding code in Table 2 by 1.5 dB. In the case of n_R=4 and n_T=2, the 4-state code of Table 2 outperforms the 4-state code of Table 1 by about 2 dB. The 16-state STTC of Table 2 outperforms the 16-state code of Table 1 by 0.5 dB. In Figure 3.19 we present the performance of the 8 and 32-state codes in Tables 1 and 2 designed by Tarokh et al and Chen et al., respectively, for a system with n_T=2 and n_R=1 and 4. In the

case of n_R=1 we see that the 8-state code from Table 1 outperforms the 8-state code from Table 2 by 0.9 dB.

In the case of 32-state codes, the code from Table 2 performs worse than code from Table 1 by approximately 1.25 dB. As before the n_R=1 codes designed using the EDC perform worse than the codes designed using the RDC [21]. In the case of n_R=4, the 8-state code in Table 2 outperforms the corresponding code in Table 1 by 0.5 dB. In addition, the 32-state code of Table 2 outperforms the 32-state code in Table 1 by 0.9 dB.

Figure 3.20 shows the performance of the 4 and 16 state codes of Tables 2,5 and 6 in a system with n_R=1 and n_R=4. In the case of n_R=1, the 4-state codes with n_T=3 and 4 perform worse than those with n_R=2. In [21] it was also found that the 4-state STTCs over Rayleigh fading channels perform worse when n_T is increased from two to three and from three to four, respectively. Even when n_R is increased from one to four as shown in Figure 3.21, the performance does not improve [21]. Also the results in Figures 3.20 and 3.21 show that over Nakagami fading channels, the 4-state code performance degrades as n_T increases. In Figure 3.21 we found that even when we increased n_R to four the performance did not improve. For the 16–state code in Figure 3.20 we found that for n_R=1, performance degrades when n_T is increased from two to three and from three to four. In Figure 3.21 we see that for n_R=4, 16-state STTCs show a 0.8 dB improvement when n_T is increased from two to three and a 0.1 dB improvement when it is increased from three to four.

Figures 3.22 and 3.23 present the performance of the 8 and 32 state codes with n_T=2,3 and 4 and n_R=1 and 4, respectively. From Figure 3.22, we see that the performance of the 8-state STTCs degrades as we increase n_T from 2 to 3 and from 3 to 4. On the other hand for the 32-state STTCs, for n_T=2 and n_T=3 the performance is approximately same. But for n_T=4 we see 32-state STTC codes shows a slight improvement than the others. In the case of n_R=4 in Figure 3.23 we see that the 8-state code shows 0.5 and 0.45 dB gains when we

increase n_T from two to three and from three to four, respectively. The 32-state code shows 0.6 and 0.5 dB gains when n_T is increased from two to three and three to four, respectively. The worse performance of STTCs from Table 5 and 6 than the codes from Table 2 is also reported in [21]. From the Tables 5 and 6 we see that the codes do not have full rank ($r = n_T$). It is mentioned in [19] [21] that the maximum value of the minimum rank of a 4-PSK STTC is min $(n_T, \left\lfloor \frac{\upsilon}{2} \right\rfloor + 1)$ [19]. Thus we can understand that the full rank can be achieved only with the memory order (υ) not less than 4 and 6, respectively [21]. As mentioned earlier that if $rn_R < 3$, Euclidean distance does not dominate the code performance [19]. This is the reason for worse performance of 4, 8 and 16-state STTCs from Table 5 and 6 than the codes from Table 2 for $n_R = 1$.

3.4.2 Correlated Fading

In this section we show the effects of transmit antenna correlation on the performance of different STTCs. In Figures 3.24 and 3.25 we give the performance of the 4-PSK 4-state STTCs designed by Tarokh et al. (Table 1) and Chen et al. (Table 2), respectively. First we assume that the signals from the two transmit antennas to the j-th ($j = 1,2$ and 4) receive antenna are correlated. We consider the three different correlation coefficients ($\rho = 0.5$, 0.8 and 1.0). Figure 3.24 shows the performance of the 4-state 4 PSK STTC codes from Table 1 in correlated Nakagami fading with different correlation coefficients. We found that with $n_R = 1$ for the values of $\rho = 0.5$, 0.8 performance is 1.75 dB and 2.75 dB worse, respectively than the uncorrelated channel. The case with $\rho = 1.0$ has the worst performance, as expected. In Figure 3.24 we see that for $n_R = 2$ code performance is degraded by 1 dB, 2 dB and 3.5 dB from the uncorrelated channel for $\rho = 0.5, 0.8$ and 1.0 respectively. For $n_R = 4$ performance (coding gain) is degraded by 0.9, 1.5 and 2.0 dB from the uncorrelated channel for $\rho = 0.5, 0.8$ and 1.0, respectively. Therefore receive diversity significantly reduces the effects of correlated fading.

Figures 3.25, 3.26 and 3.27 show the performance of the 8,16 and 32-state STTCs of Table 1, respectively. From these figures we found that as we increase the number of states the effect of fading correlation reduces. It is also evident that with more receive antennas in the system better performance is achieved over correlated fading channels. In the case of a 32-state STTC with n_R=4 and n_T=2 we found from Figure 3.27 that the performance for the case of ρ=0.5 and 0.8 is worse than with no correlation by about 1 dB. In the case of severe transmit correlation (ρ=1.0) performance is degraded by 2 dB from the uncorrelated channel. This result is similar to that observed in Figure 3.24.

Figure 3.28 presents the performance of the 8-state 8-PSK Table 1 over a correlated Nakagami fading channel for ρ=0, 0.5,0.8 and 1. Figure 3.29 shows the performance of the 16-state 8-PSK code from Table 1 in a correlated fading channel with ρ = 0 and 0.5. We see that the 8-PSK STTC code follows the same trend as for the 4 PSK STTCs over correlated Nakagami fading channels. For a single receive antenna, the effect of correlated fading performance is severe. For n_R=4 and ρ=0.5 we see that the performance of the 8-state STTC degrades by 0.8dB from the case of uncorrelated channels. For the case of n_R=4 and ρ=0.5, performance of the 16-state STTC degrades by 0.25 dB from the case of uncorrelated channels. So as we increase the number of states the effect of the correlation reduces. Figures 3.30 to 3.33 show the performance of the 4, 8,16 and 32-state STTCs over correlated Nakagami fading channels for ρ = 0, 0.5, 0.8 and 1.

If we compare the performance of the 4-state codes of Figure 3.30 with that in Figure 3.24, we see that for n_R=2, the 4-state code from Table 2 performs better than the code from Table 1. For n_R=4 and ρ=0.5, the 4-state code from Table 2 outperform the code from Table 1 by about 2 dB. For n_R=4 and ρ=1, the 4-state code from Table 2 outperform the code from Table 1 by about 1dB. Now comparing Figures 3.33 and 3.27 we see that for n_R=2 and ρ=0.5, the 32-state code from Table 2 outperform the code from Table 1 by about 1 dB. For n_R=4 and ρ=0.5, the 32-state code from Table 2 outperform the code from Table 1 by about 1.5 dB. This shows over correlated fading channels, with large receive

diversity, the STTCs designed using the EDC (Table 2) show significant performance improvements over the codes designed using the RDC (Table 1).

3.4.3 Summary

From our results we found that the performance of STTC designed by EDC performs worse than the codes designed by RDC in a system with n_T=2 and n_R=1. However in the same system when we employ multiple receive antennas (n_R=2,4) the STTCs designed by EDC outperform the STTCs designed by RDC. This performance trend is also observed in Rayleigh fading channels.

When we increase the number of transmit antenna from n_T=2 to 3 and 4 in a system with n_R=1, the performance of the 4,8 and 16 states codes designed by EDC degrades. Only the 32-state code showed any performance improvement. As we increase the number of receiver antennas from 2 and 4 we see that the system shows much better performance. As already mentioned in a Rayleigh fading channel, when we increase the number of transmit antennas we do not get more diversity gain for fixed n_R.

We found that the performance of STTCs over correlated Nakagami fading channels degrade, as the correlation increases. However, when multiple receive antennas are employed correlation degradation is reduced. With multiple receive antennas, the codes designed by EDC perform better than the codes designed by RDC.

3.5 Summary

In this Chapter we provided simulation results for the STTC proposed by Tarokh et al. and Chen et al. over different fading channels. In Section 3.1 we provided a short discussion of the simulation parameters and simulation methods. In Section 3.2 we presented the performance of different STTCs over Rayleigh fading channels. In Section 3.3 we showed the performance of the STTCs of Table 1 and Table 2 over Ricean fading channels. In Section 3.4 we provided a detailed performance comparison of these codes over independent and correlated Nakagami fading channels. Earlier in our discussion we mentioned that the Nakagami fading channel is more flexible than the Rayleigh and Ricean channels [3]. For

this reason we presented more results on the performance of STTCs over Nakagami channels. It was determined that the design criteria for space-time trellis codes over Rayleigh fading channels is suitable for both independent and correlated Nakagami fading channels. Our simulation results show that the 4,8,16 and 32-state codes from Table 2 perform worse than the codes from Table 1 for n_T=2 and n_R=1 over Nakagami fading channels. However for n_T=2 and n_R=2 and 4 the codes from Table 2 outperform the codes from Table 1. We also observed that when we have a system with n_T=2 and n_R=1 and we increase the number of transmit antennas, the codes designed by EDC for n_T=3 and 4 perform worse than the codes designed for n_T=2.

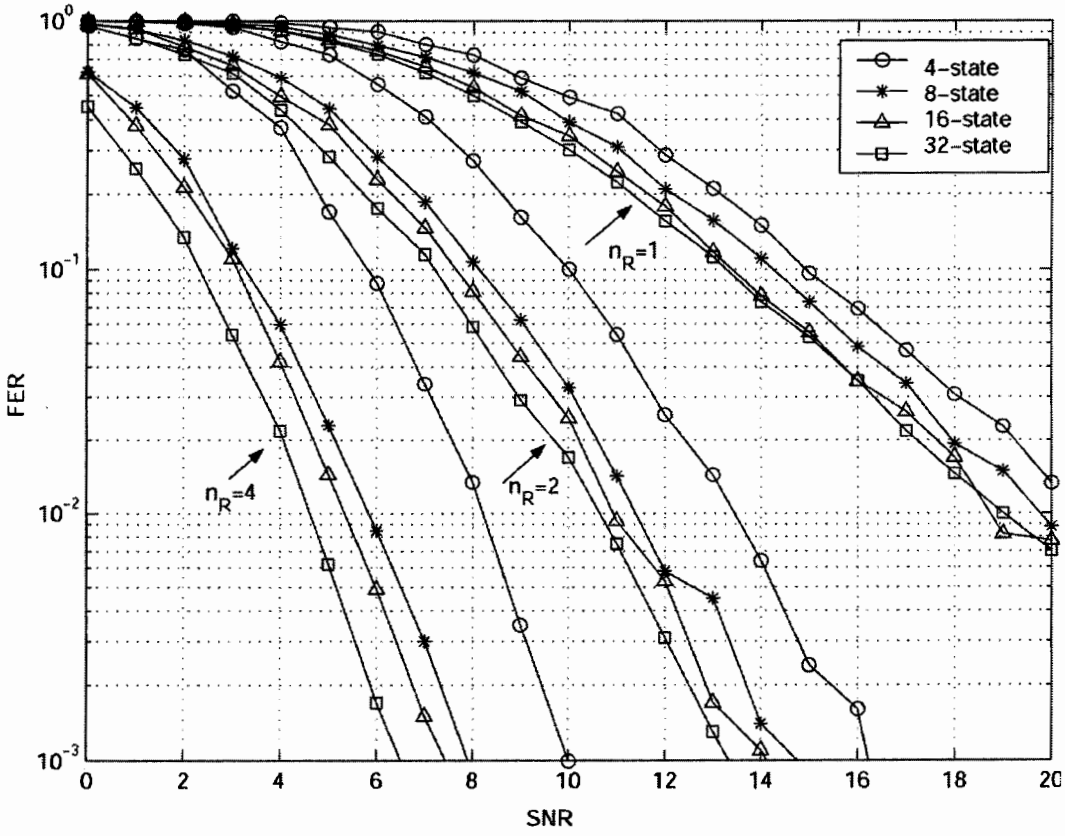

Figure 3.1: Performance comparison of the 4-PSK STTCs from Table 1 (Tarokh et al.) over Rayleigh fading channels with n_T =2 and n_R =1, 2 and 4.

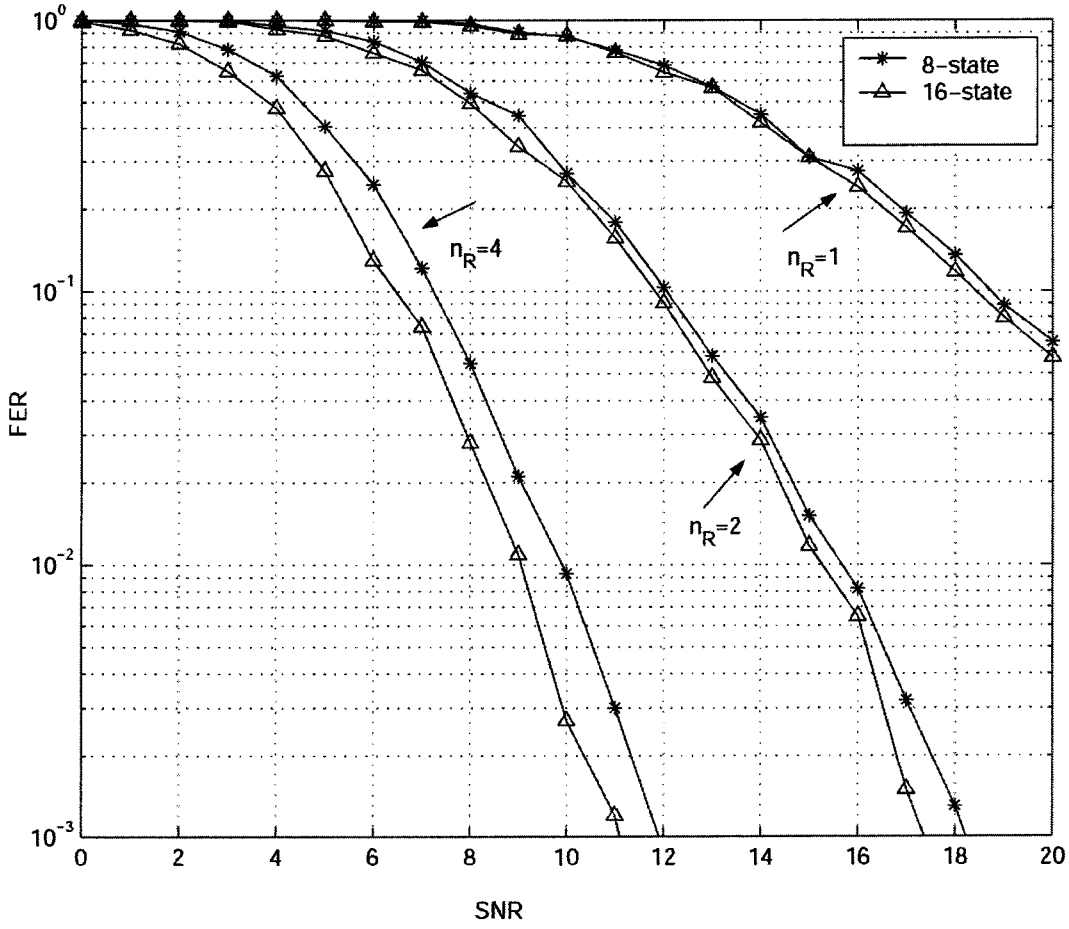

Figure 3.2: Performance comparison of the 8-PSK STTCs from Table 1 (Tarokh et al.) over Rayleigh fading channels with n_T =2 and n_R =1, 2 and 4.

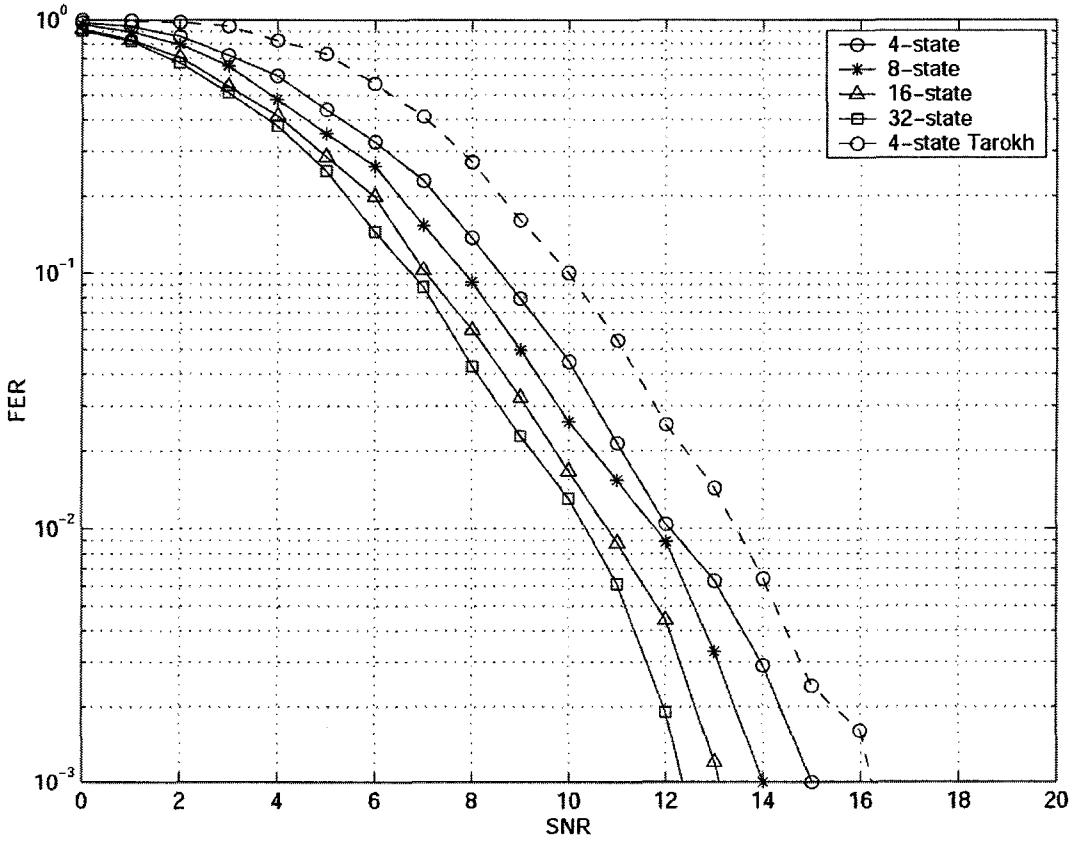

Figure 3.3: Performance comparison of the 4-PSK STTCs of Table 2 (Chen et al.) over Rayleigh fading channels with n_T =2 and n_R = 2.

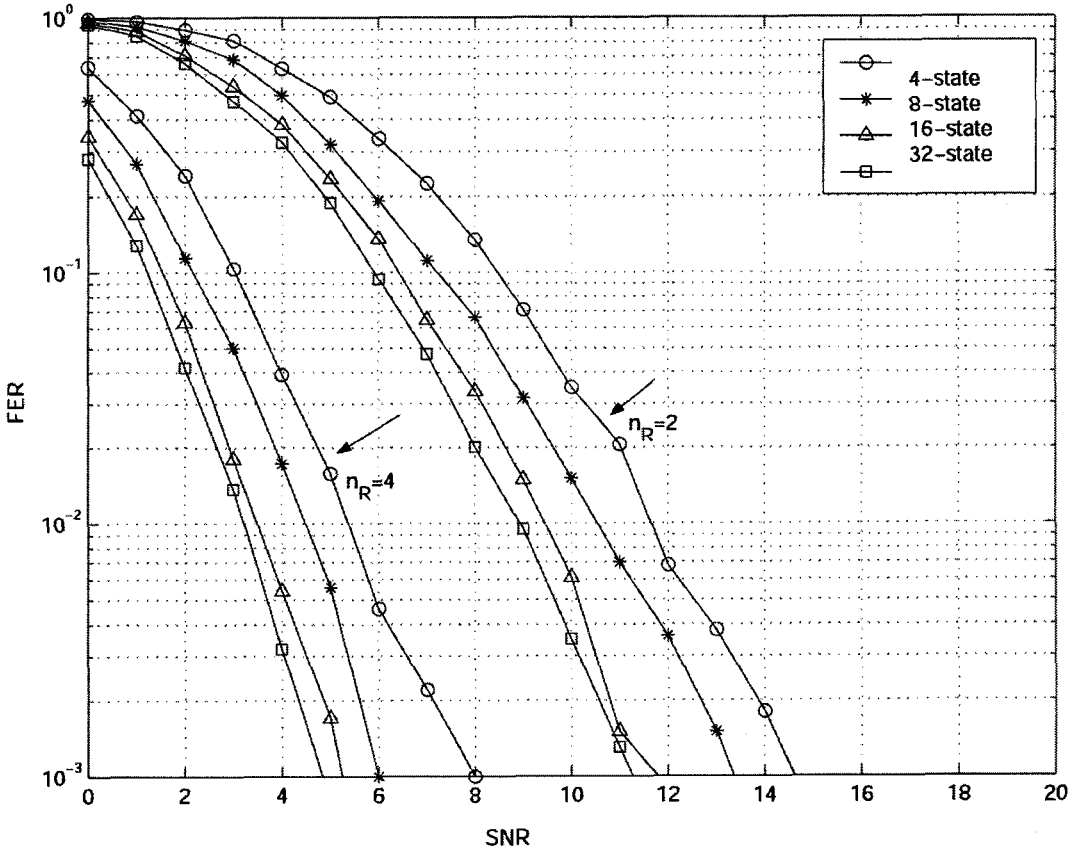

Figure 3.4: Performance comparison of the 4-PSK STTCs from Table 5 (Chen et al.) over Rayleigh fading channels with n_T =3 and n_R = 2 and 4.

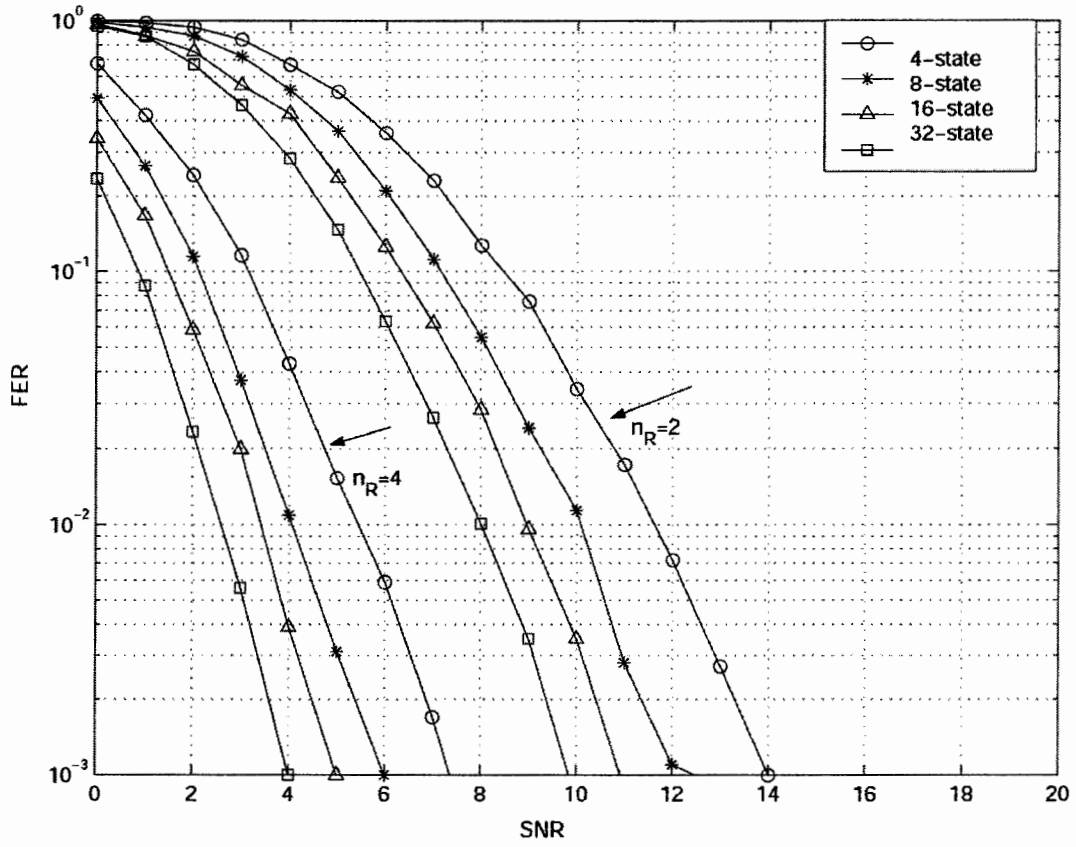

Figure 3.5: Performance comparison of the 4-PSK STTCs from Table 6 (Chen et al.) over Rayleigh fading channels with n_T =4 and n_R = 2 and 4.

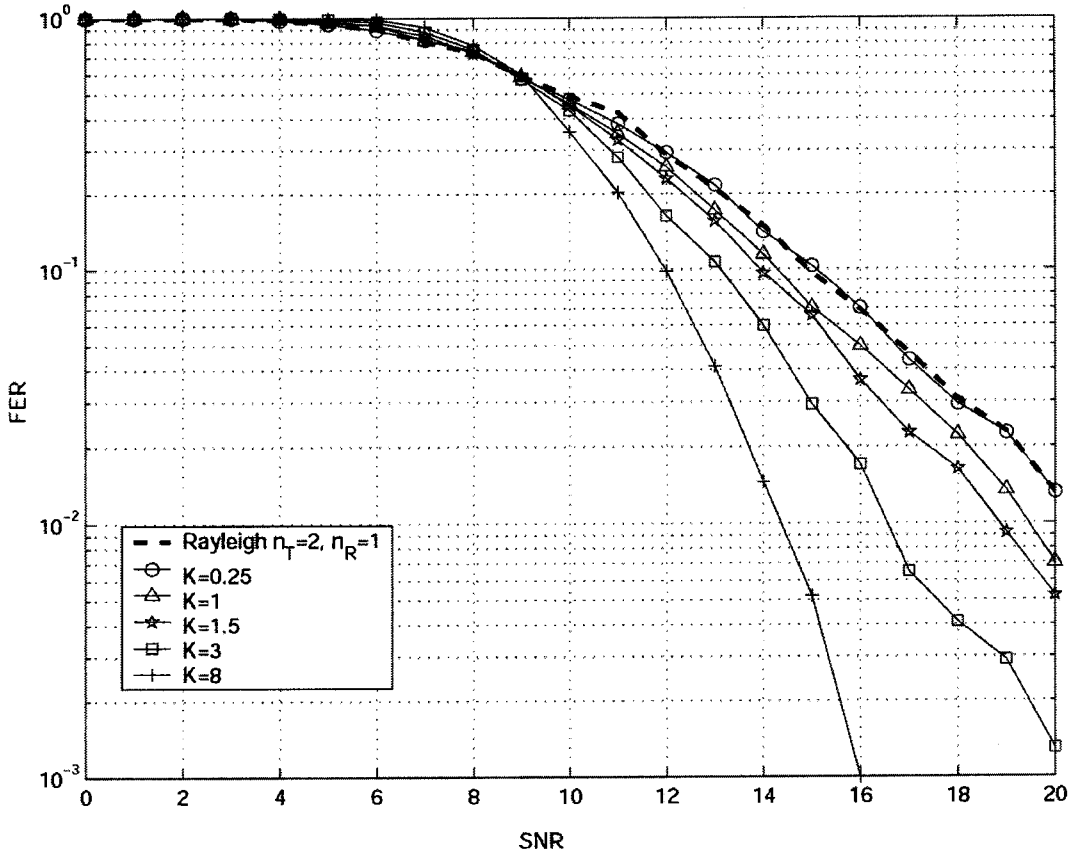

Figure 3.6: Performance of the 4-PSK STTCs from Table 1 (Tarokh et al.) over Ricean fading channels for K= 0.25, 1, 1.5, 3, 8 with n_T =2 and n_R = 1.

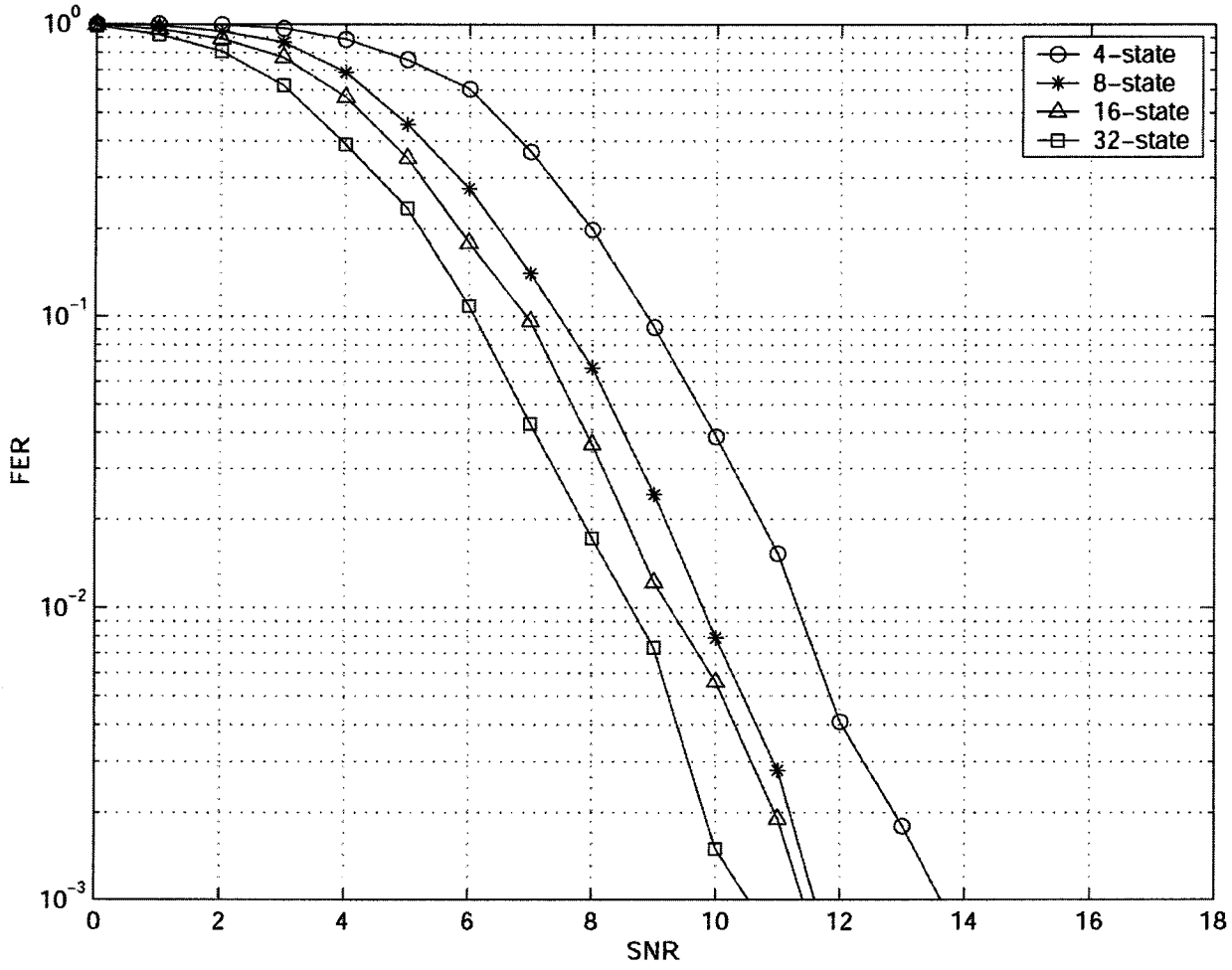

Figure 3.7: Performance of the 4-PSK STTCs from Table 1 over Ricean fading channels (K=3) with n_T=2, n_R=2.

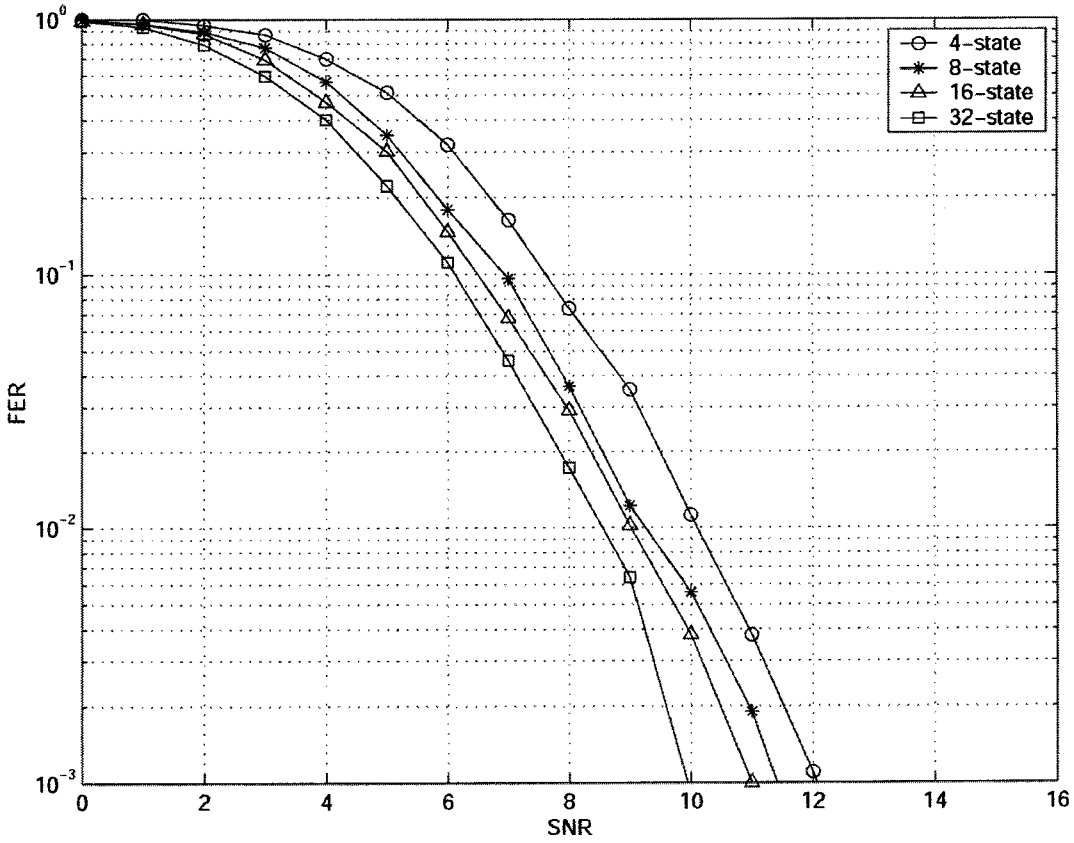

Figure 3.8: Performance of the 4-PSK STTCs from Table 2 over Ricean fading channels (K=3) with n_T=2, n_R=2.

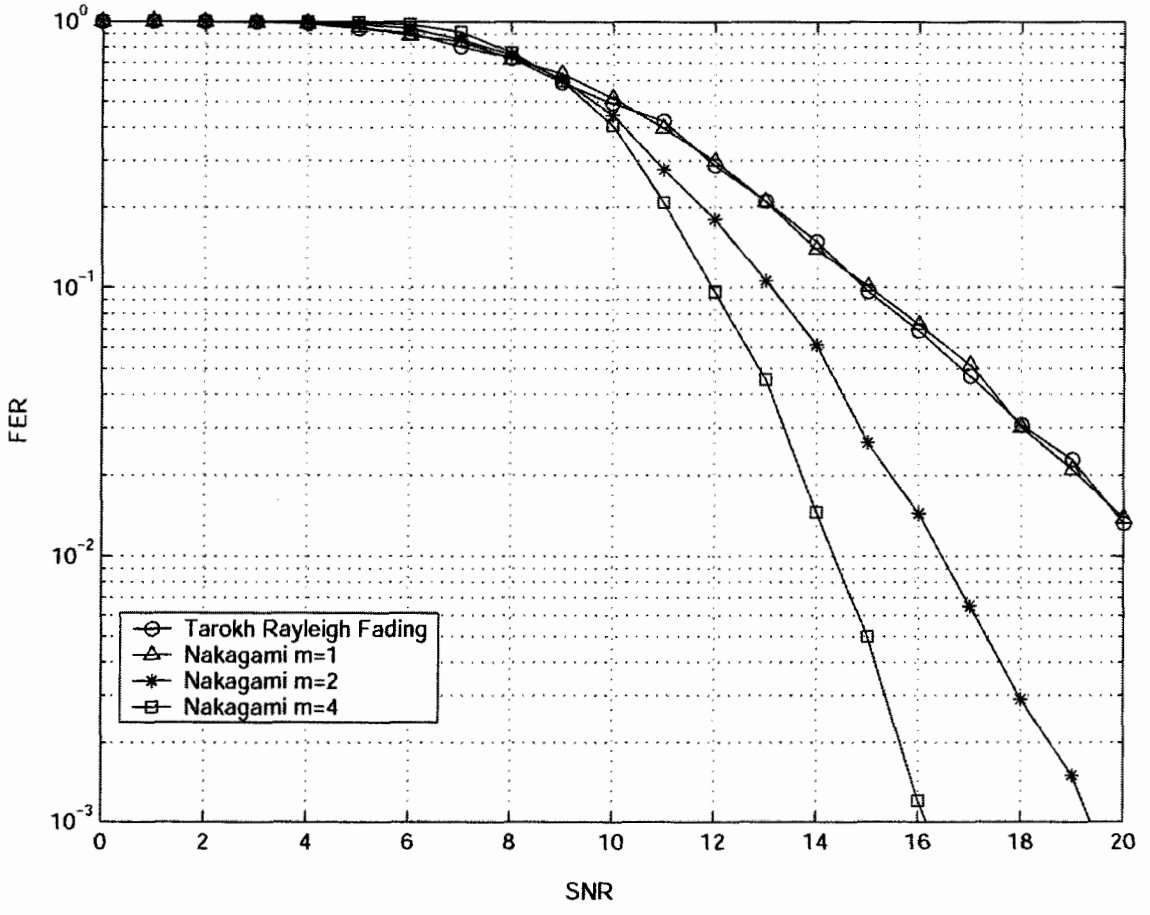

Figure 3.9: Performance Comparison of the 4-PSK 4-state STTCs from Table 1 over Nakagami fading channels for m = 1,2 and 4 with n_T =2, n_R =1.

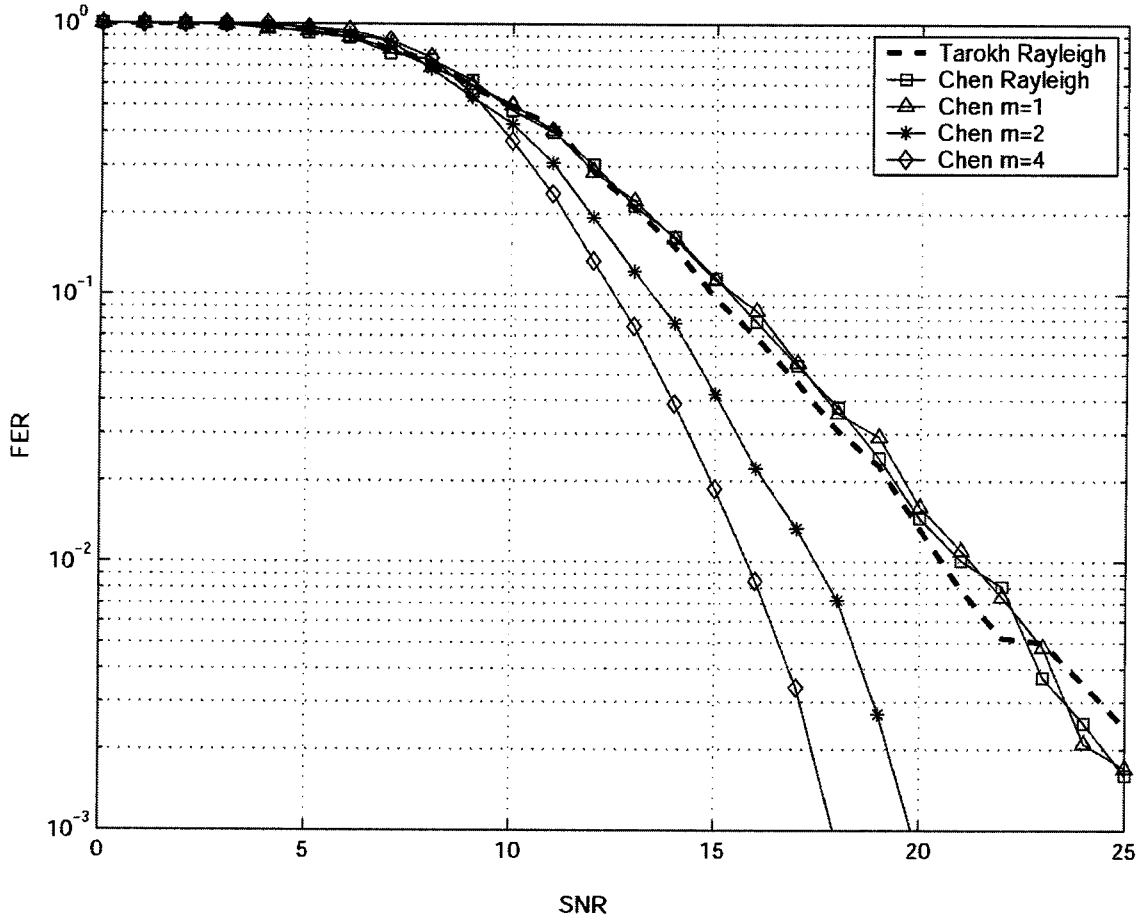

Figure 3.10: Performance Comparison of the 4-PSK 4-state STTC from Table 2 (Chen et al.) over Nakagami fading channels for m = 1,2 and 4 with n_T =2, n_R =1.

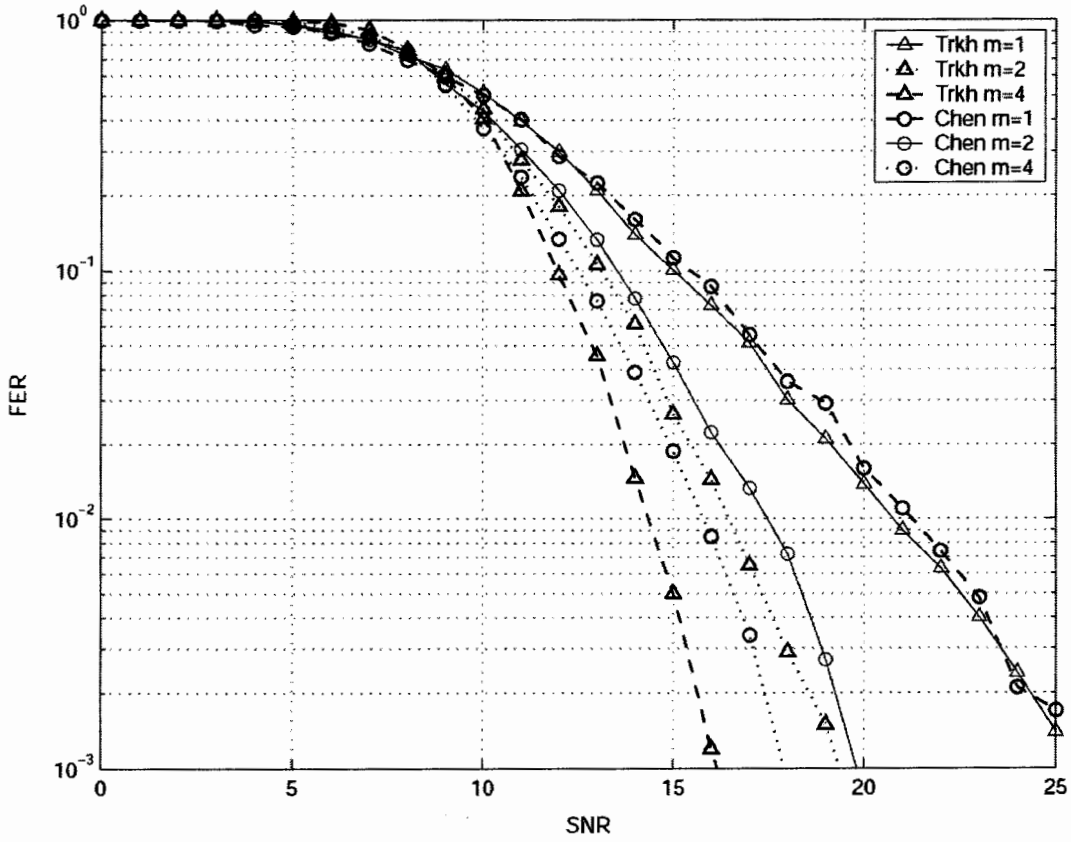

Figure 3.11: Performance Comparison of the 4-PSK 4-state STTC from Table 1 and Table 2 over Nakagami fading channels for m = 1,2 and 4 with n_T =2, n_R =1.

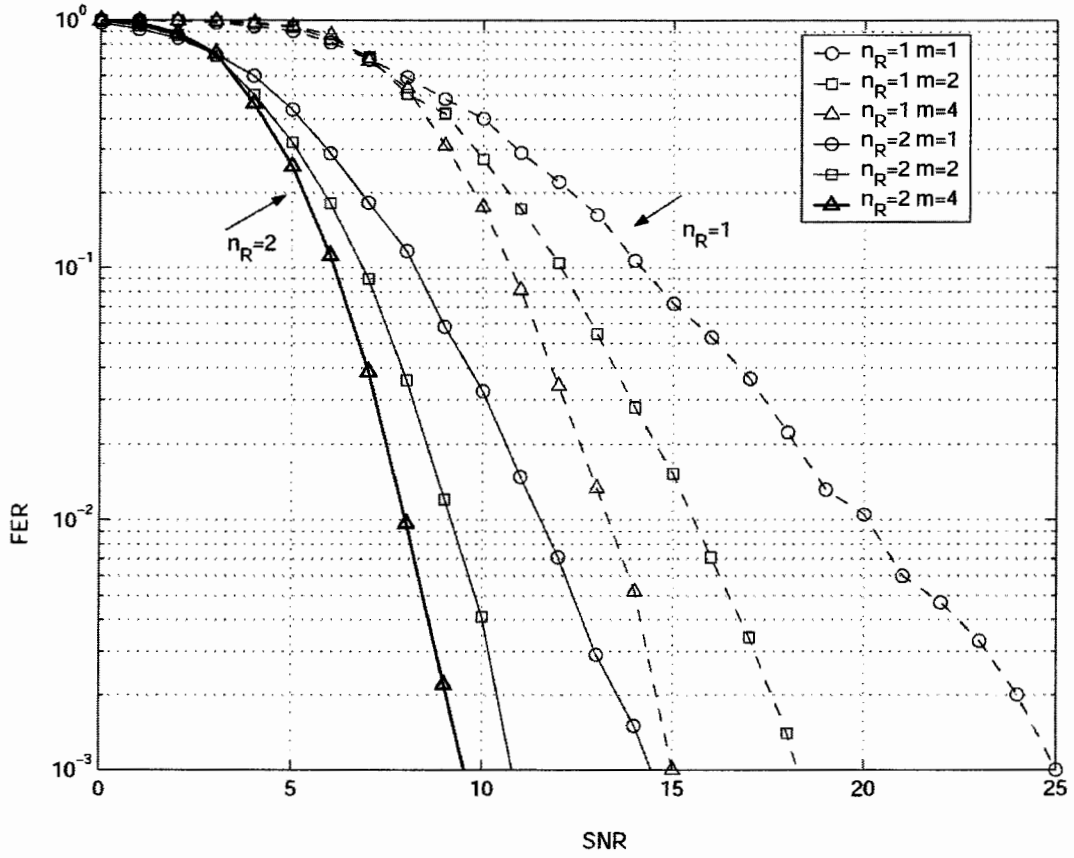

Figure 3.12: Performance of the 4-PSK 8-state STTC from Table 1 (Tarokh et al.) over Nakagami fading channels for m = 1,2 and 4 with n_T =2, n_R =1 and 2.

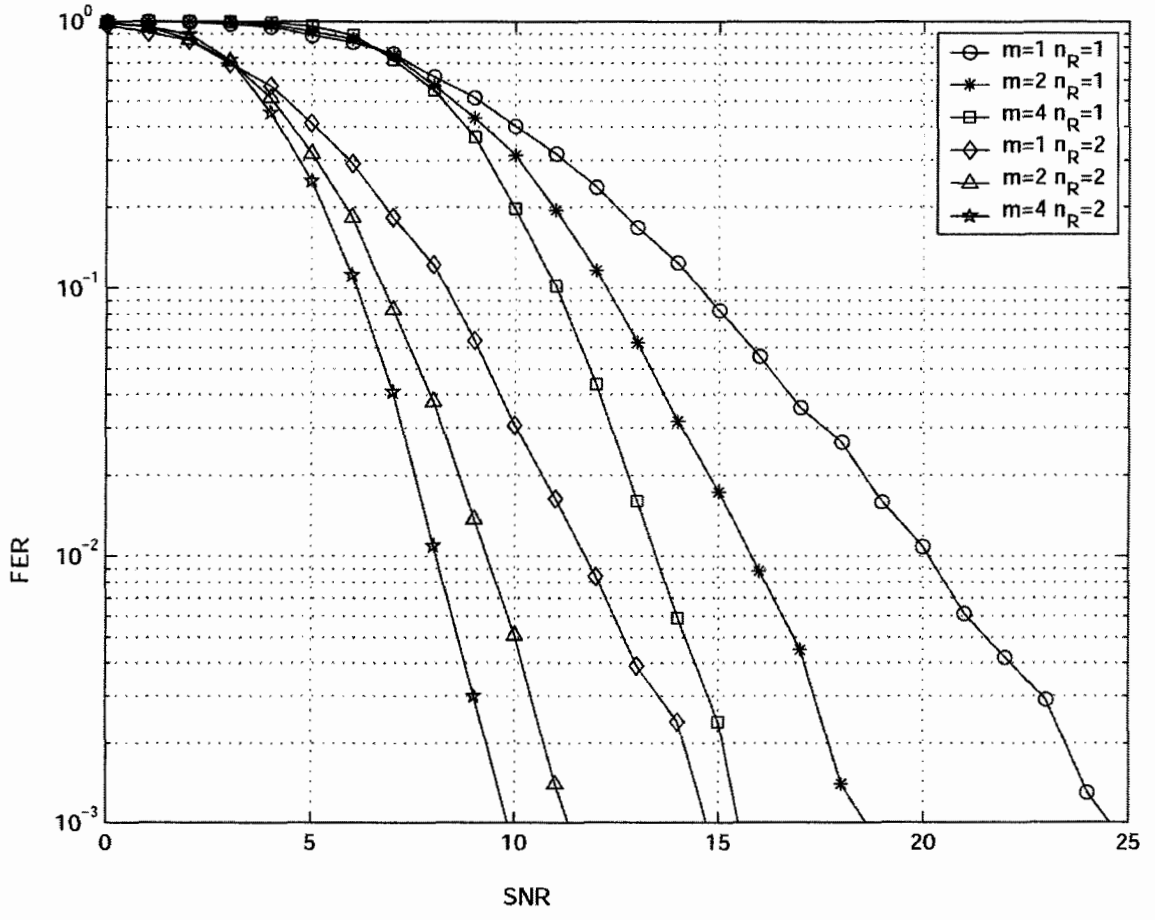

Figure 3.13: Performance of the 4-PSK 8-state STTC from Table 2 (Chen et al.) over Nakagami fading channels for m = 1,2 and 4 with n_T =2, n_R =1 and 2.

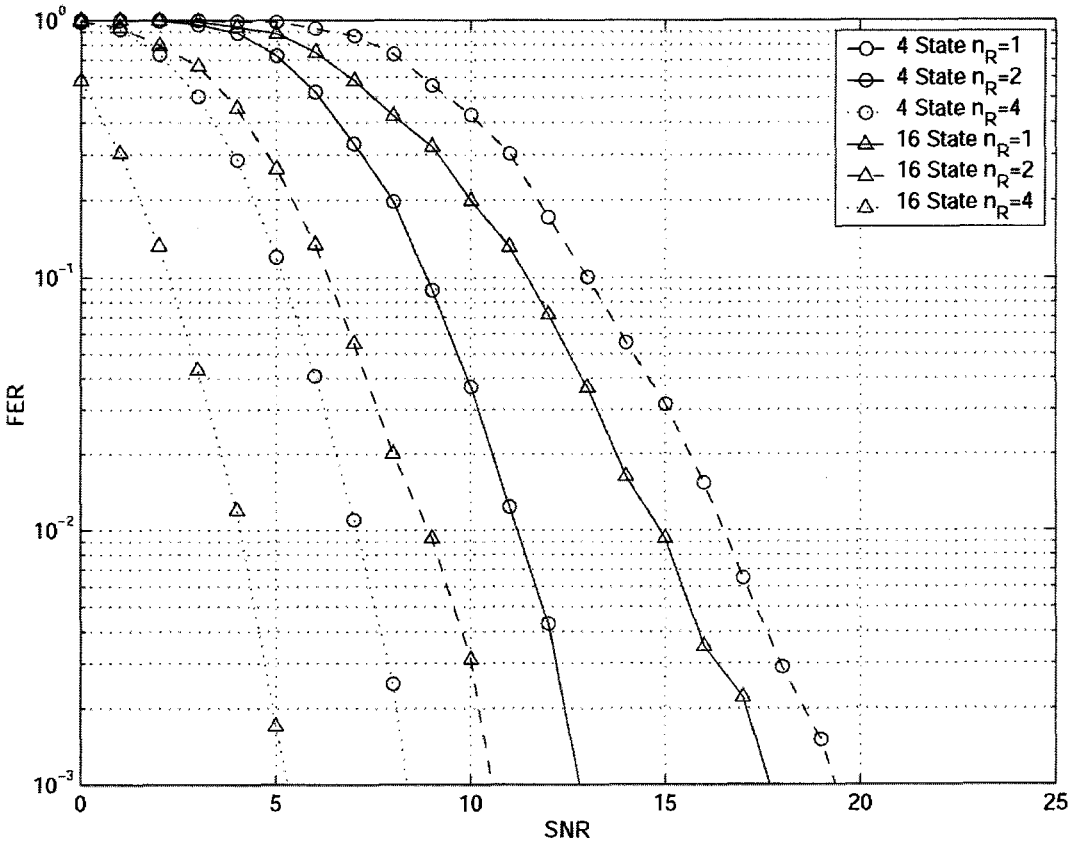

Figure 3.14: Performance of the 4-PSK 4 and 16-state STTCs from Table 1 (Tarokh et al. code) over Nakagami fading channels (m = 2) with n_R=1,2 and 4 and n_T=2.

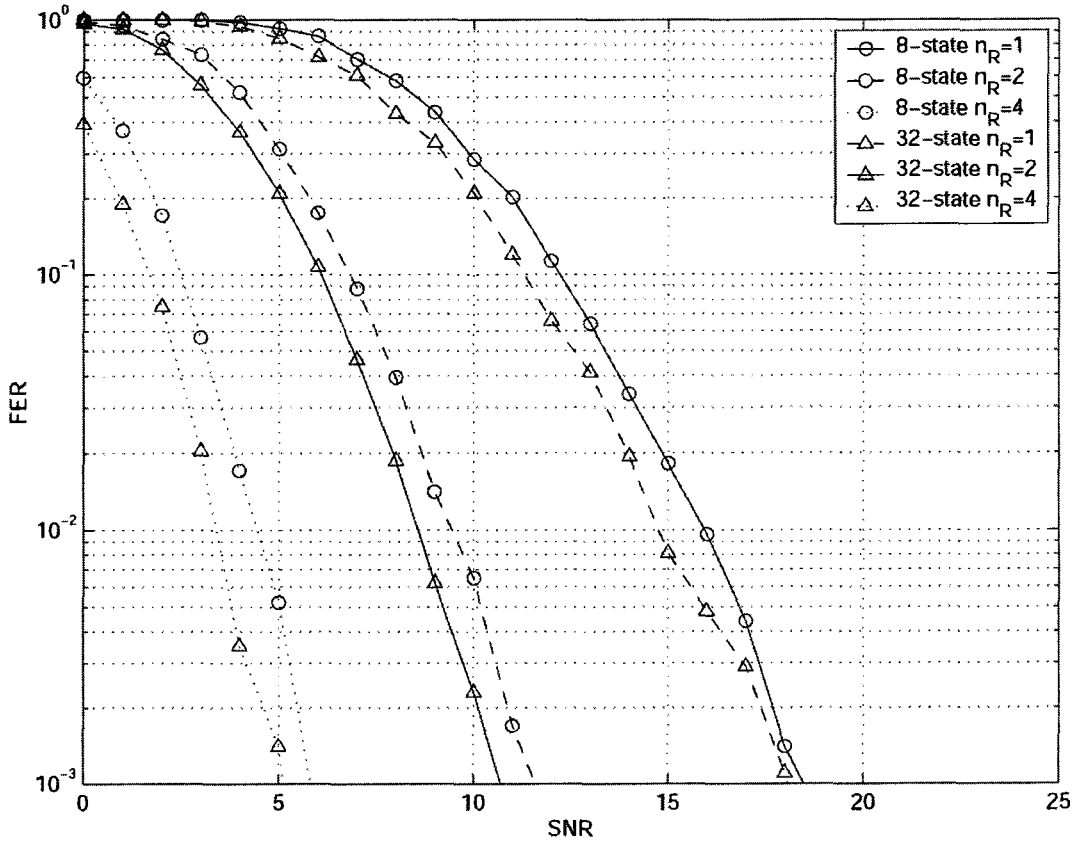

Figure 3.15: Performance of the 4-PSK 8 and 32-state STTCs from Table 1 (Tarokh et al. code) over Nakagami fading channels (m = 2) with n_R=1,2 and 4 and n_T=2.

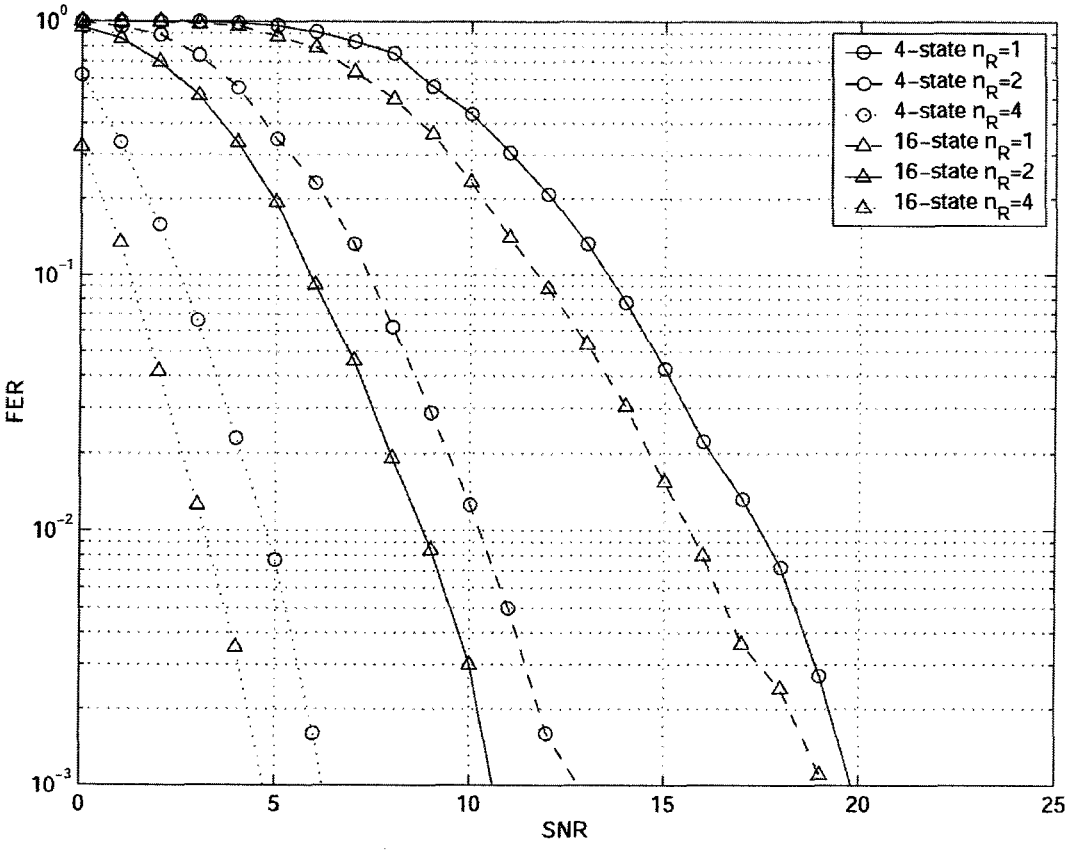

Figure 3.16: Performance of the 4-PSK 4 and 16-state STTCs from Table 2 (Chen et al.) over Nakagami fading channels ($m = 2$) with n_R=1,2 and 4 and n_T=2.

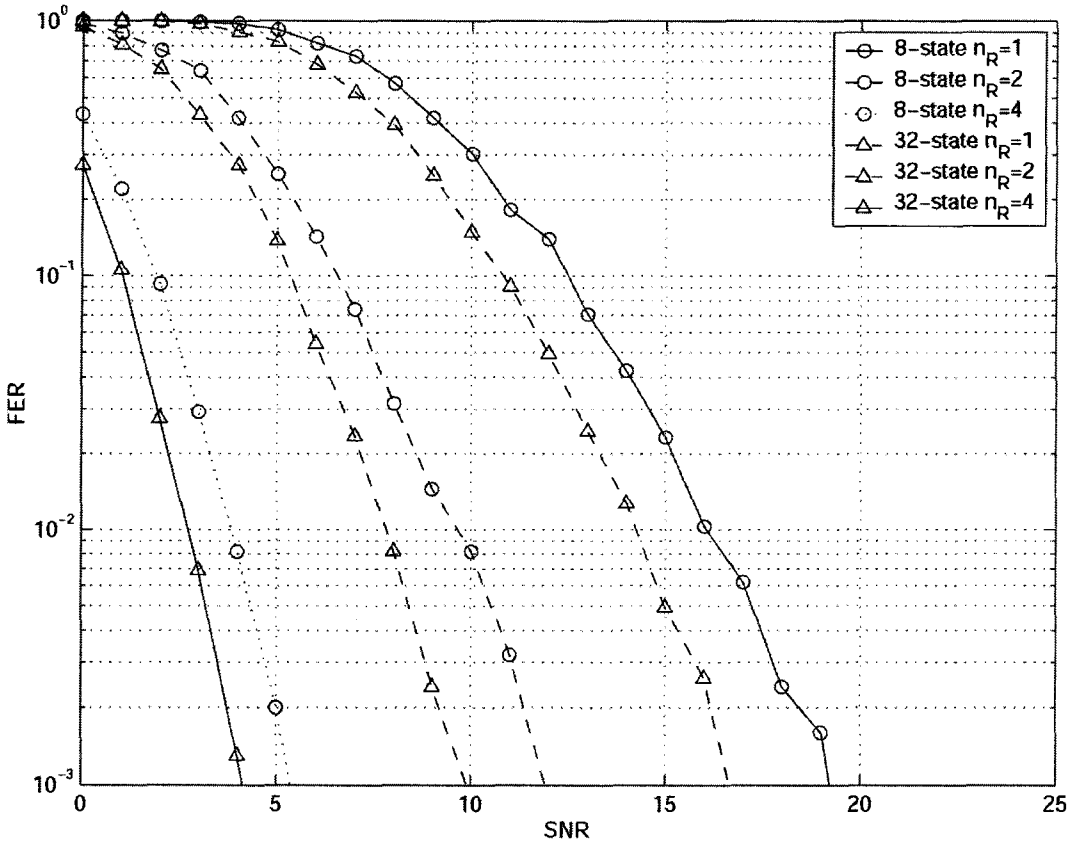

Figure 3.17: Performance of the 4-PSK 8 and 32-state STTCs from Table 2 (Chen et al.) over Nakagami fading channels ($m = 2$) with n_R =1,2 and 4 and n_T =2.

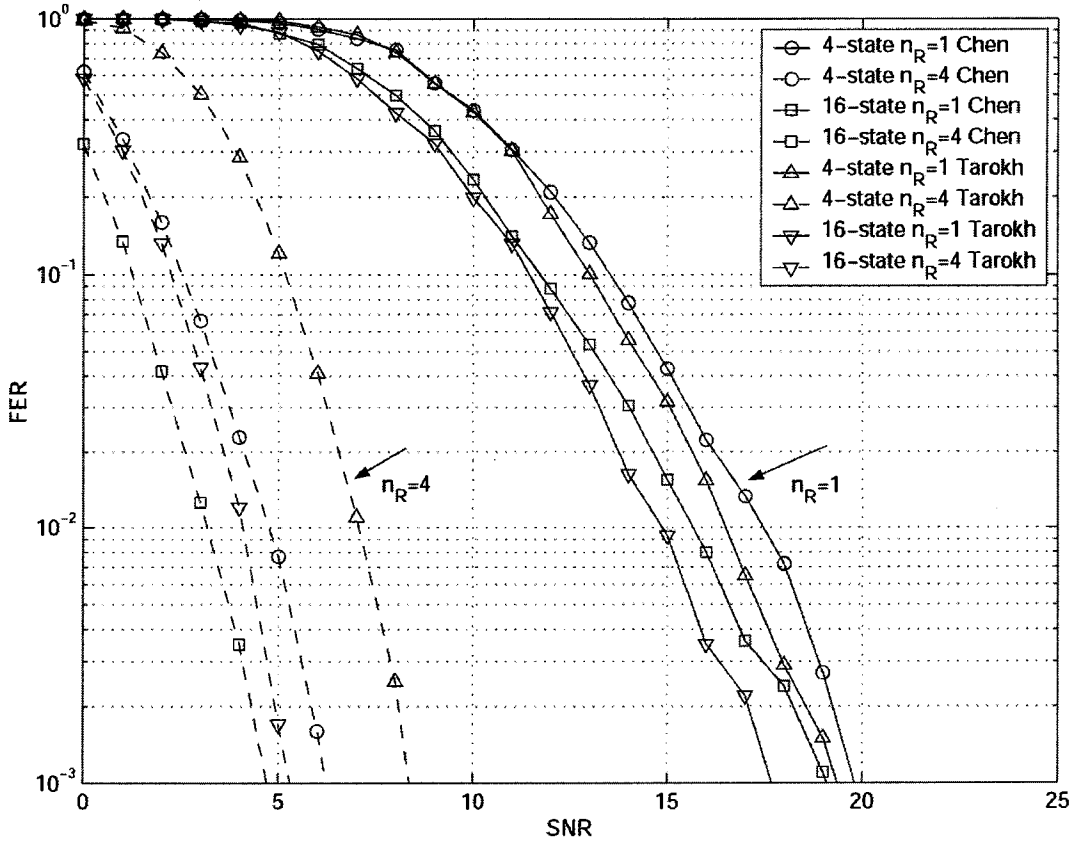

Figure 3.18: Performance Comparison of the 4-PSK 4 and 16-state STTCs from Tables 1 and 2 over Nakagami fading (m = 2) for n_R =1 and 4 and n_T =2.

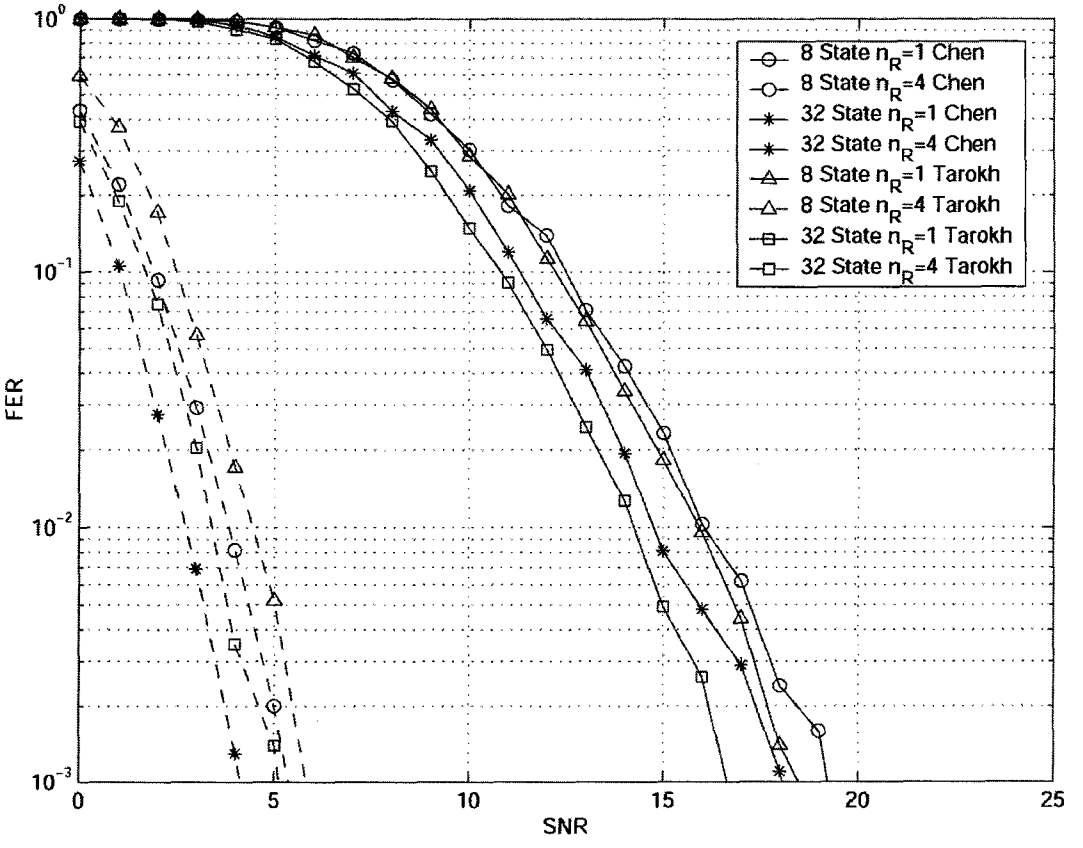

Figure 3.19: Performance Comparison of the 4-PSK 8 and 32-state STTCs from Tables 1 and 2 over Nakagami fading channels ($m = 2$) for n_R=1 and 4 and n_T=2.

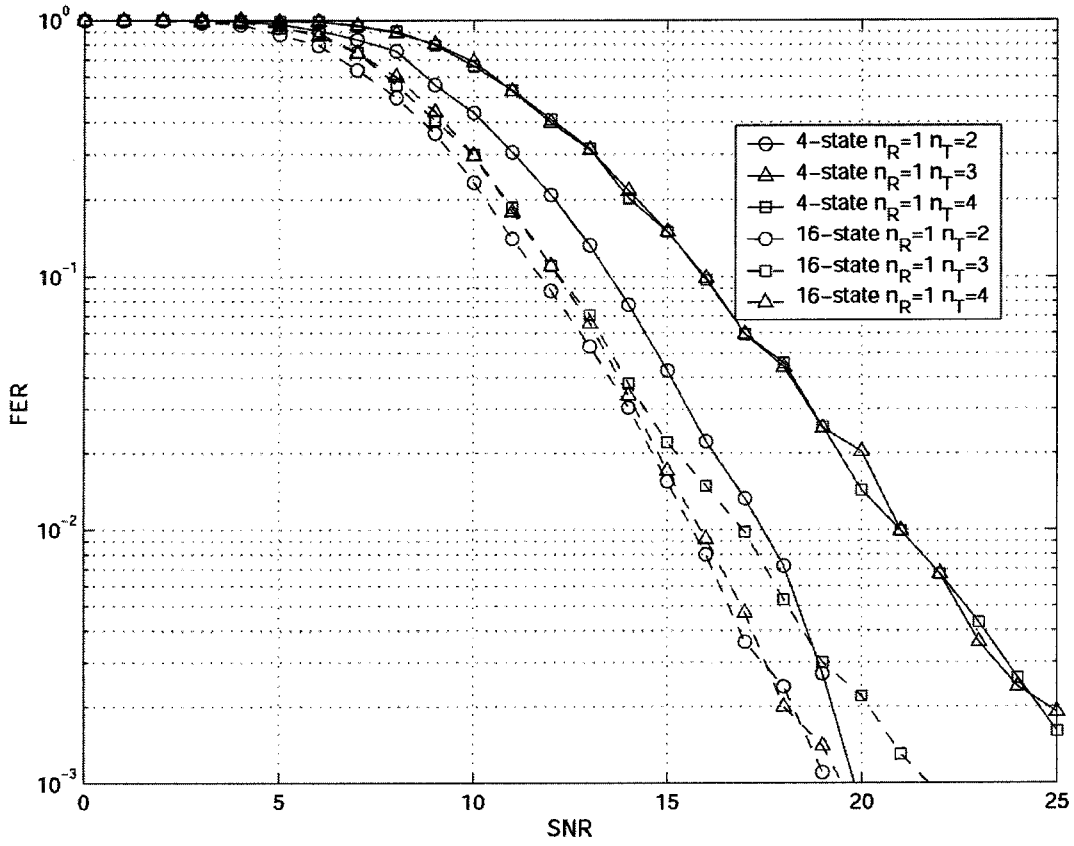

Figure 3.20: Performance comparison of the 4-PSK 4 and 16-state STTCs fromTables 2, 5 and 6 over Nakagami fading channels (m = 2) with n_R=1 and n_T=2,3 and 4.

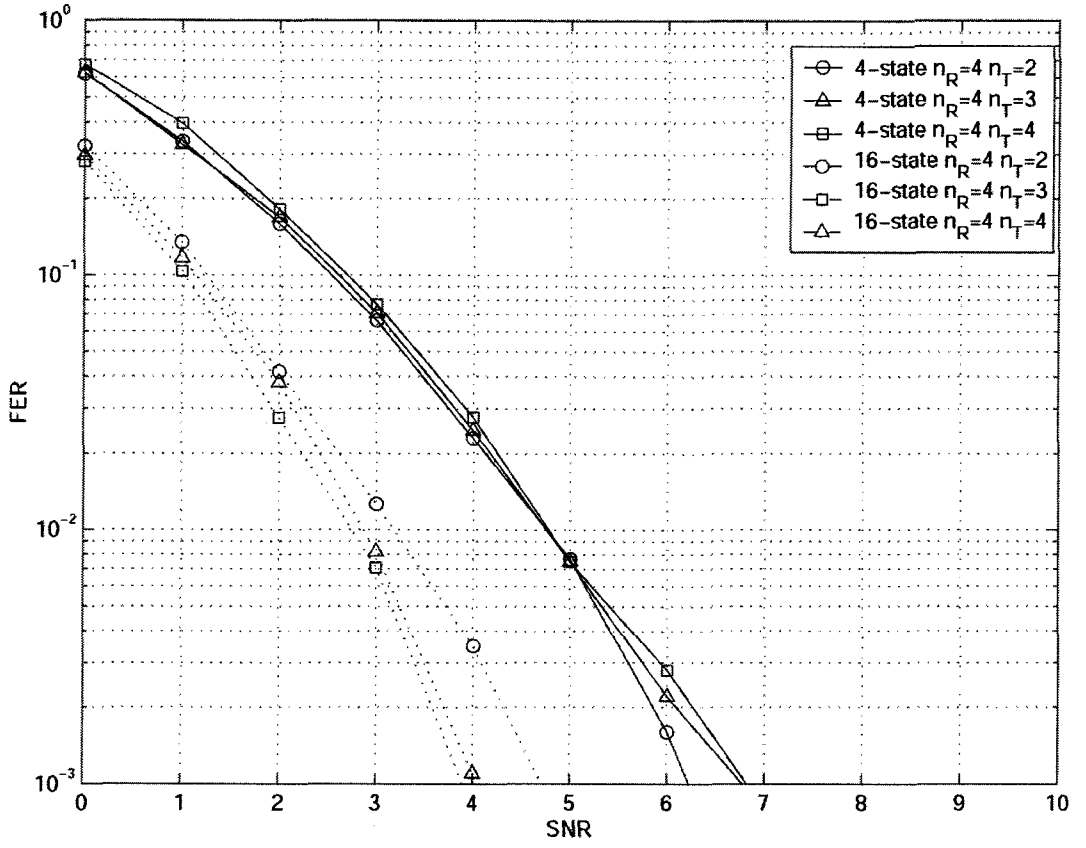

Figure 3.21: Performance Comparison of the 4-PSK 4 and 16-state STTCs of Tables 2, 5 and 6 (Chen et al.) over Nakagami fading channels with n_R=4 and n_T=2,3 and 4.

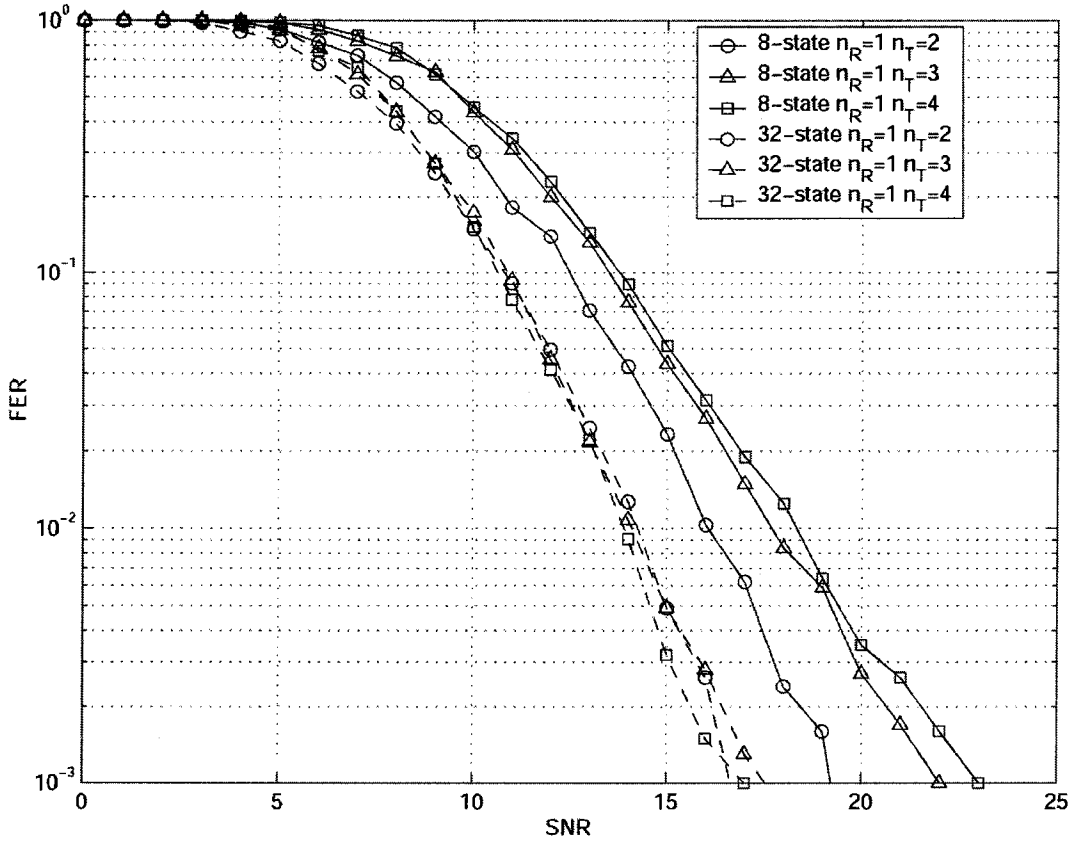

Figure 3.22: Performance Comparison of the 4-PSK 8 and 32-state STTCs from Tables 2, 5 and 6 (Chen et al.) over Nakagami fading channels (m = 2) with n_R=1 and n_T =2, 3 and 4.

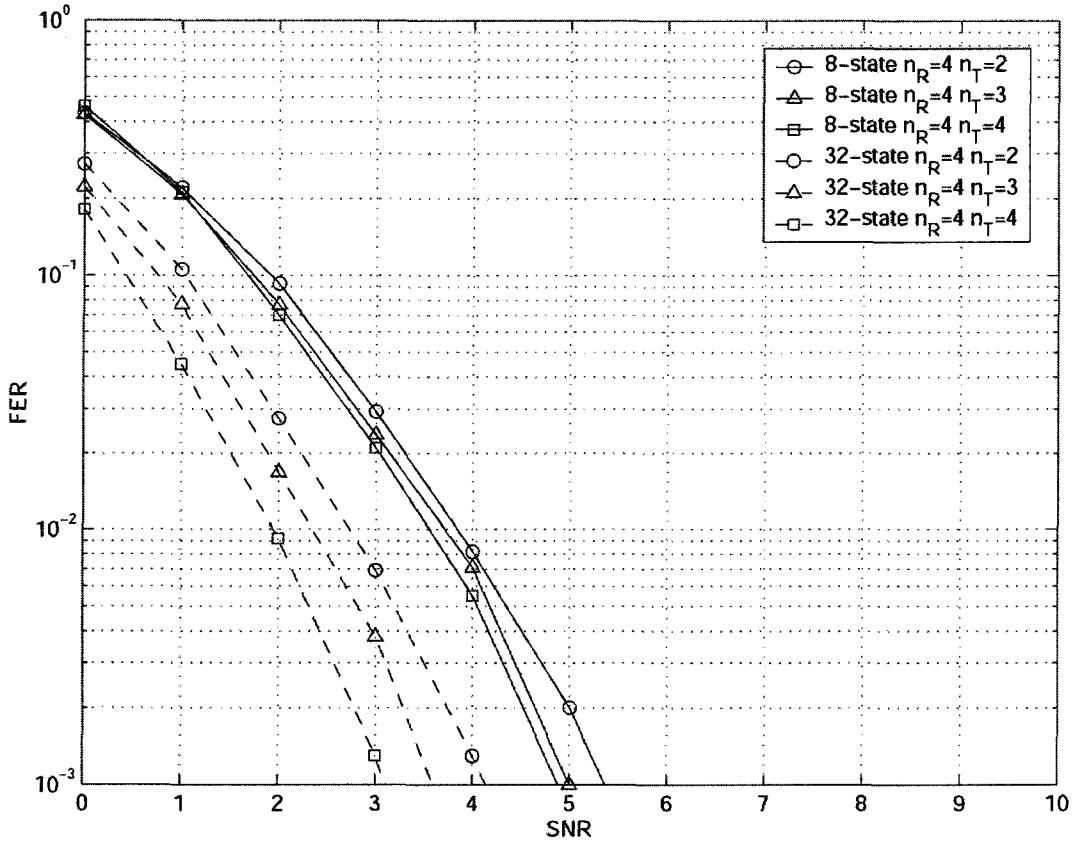

Figure 3.23: Performance Comparison of the 4-PSK 8 and 32-state STTCs from Tables 2, 5 and 6 over Nakagami fading channels ($m = 2$) with n_R=4 and n_T=2,3 and 4.

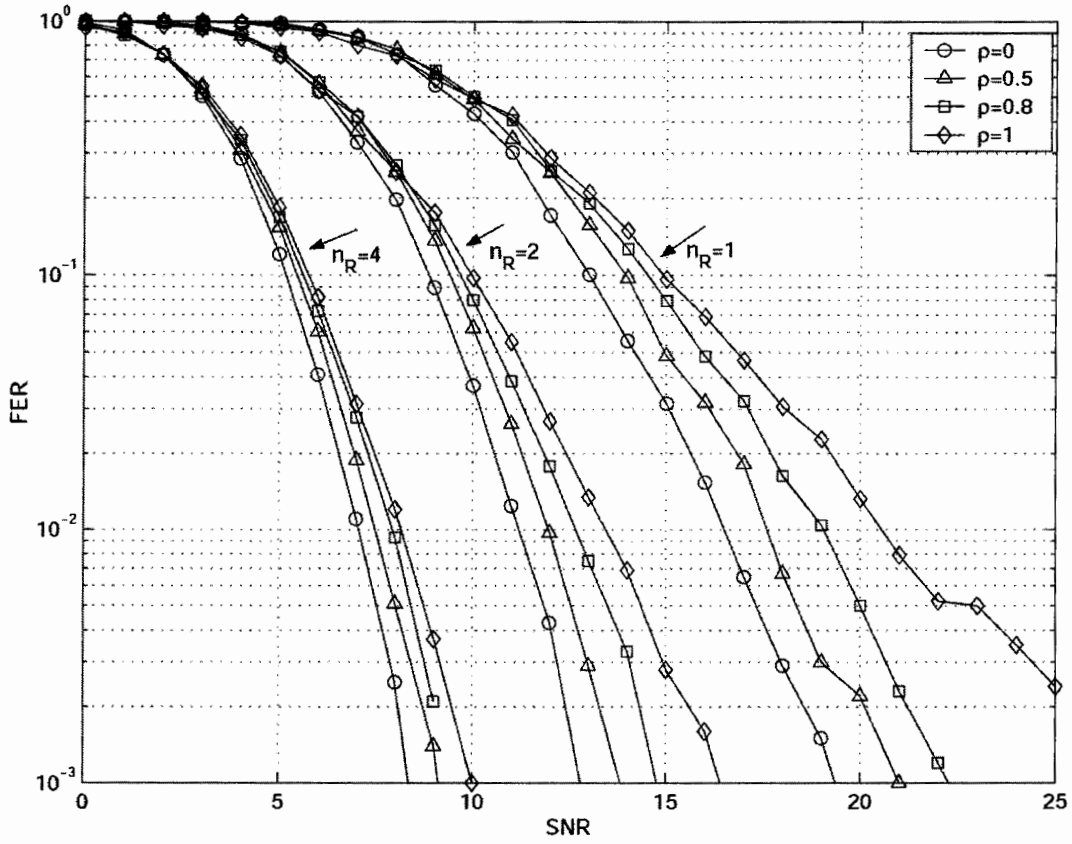

Figure 3.24: Performance Comparison of the 4-PSK 4-state STTC from Table 1 over correlated Nakagami fading channels for ρ=0, 0.5, 0.8 and 1 with n_R=1, 2 and 4 and n_T=2.

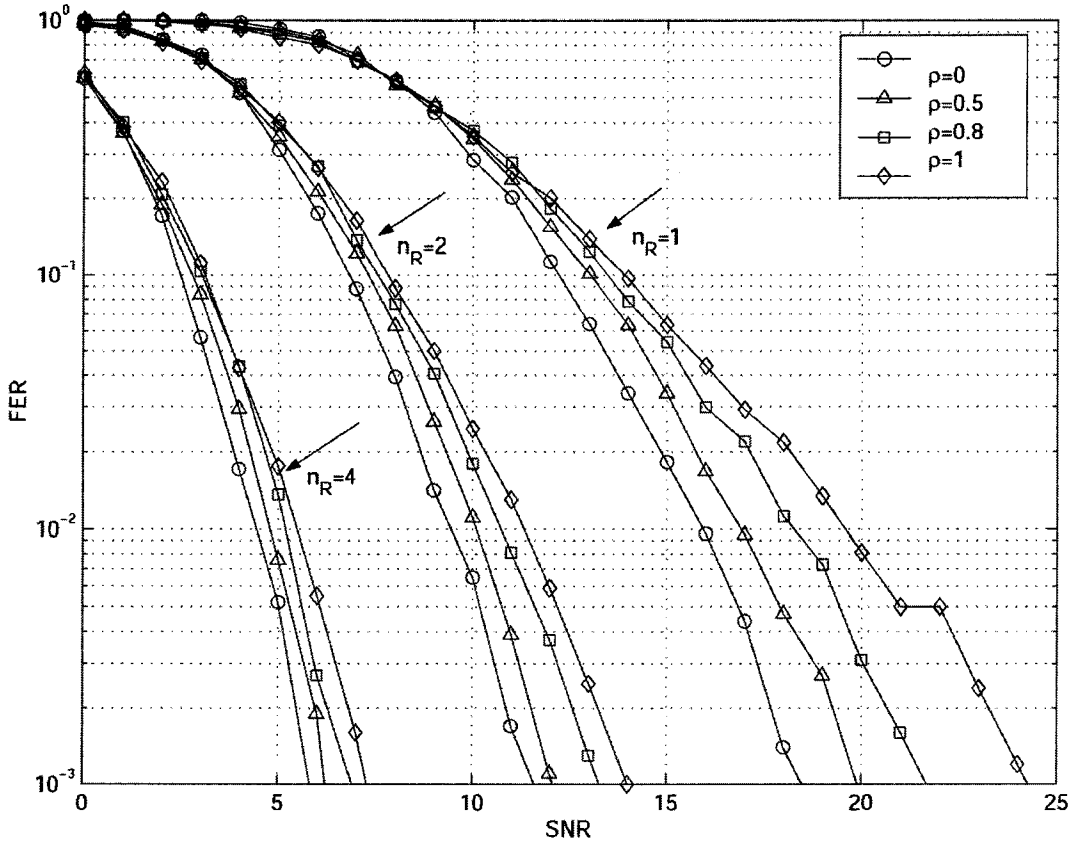

Figure 3.25: Performance Comparison of the 4-PSK 8-state STTC from Table 1 over correlated Nakagami fading channels for ρ =0, 0.5, 0.8 and 1 with n_R =1, 2 and 4 and n_T =2.

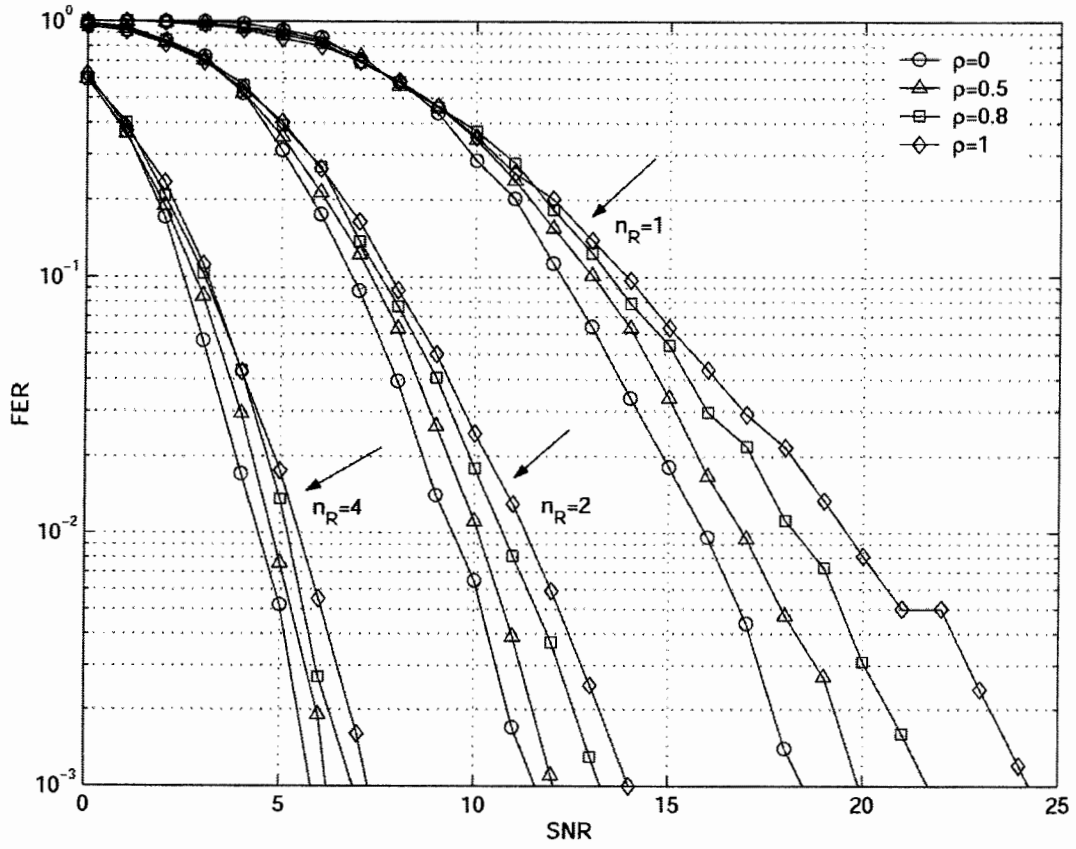

Figure 3.26: Performance Comparison of the 4 PSK 16-state STTCs from Table 1 over correlated Nakagami fading channels for ρ=0, 0.5, 0.8 and 1 with n_R=1, 2 and 4 and n_T=2.

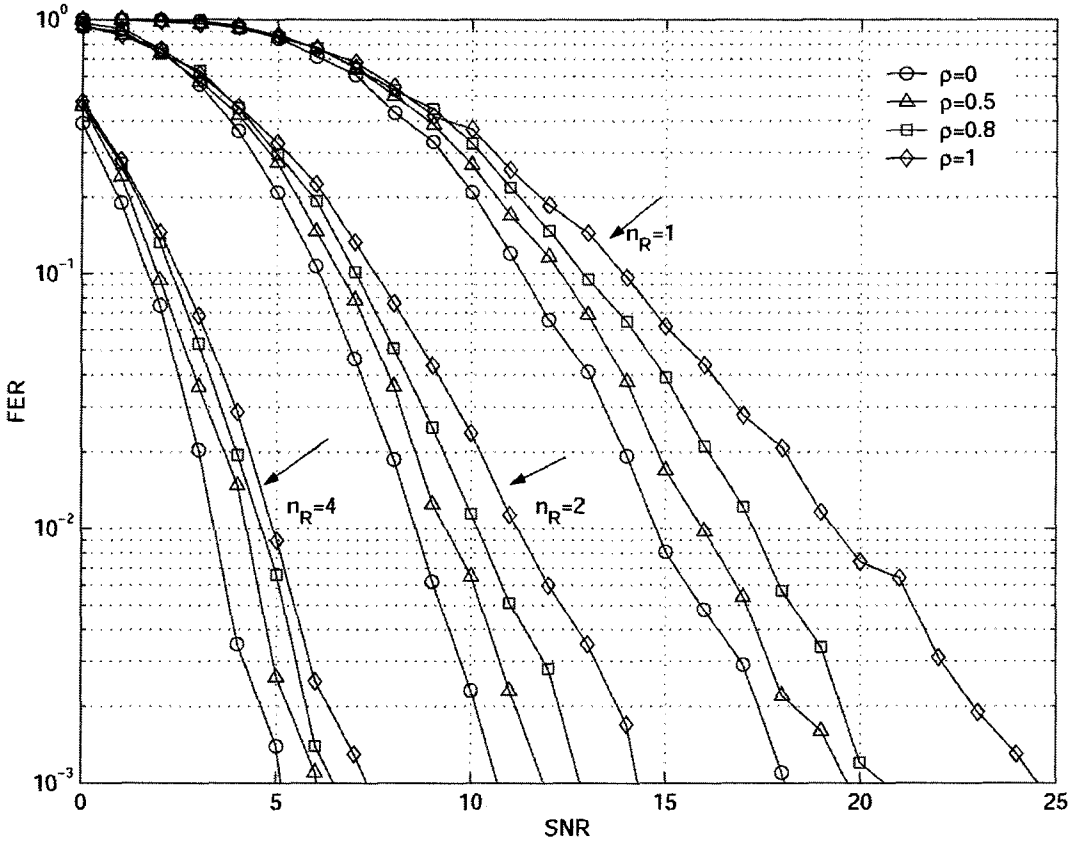

Figure 3.27: Performance Comparison of the 4-PSK 32-state STTC from Table 1 over correlated Nakagami fading channels for ρ=0, 0.5, 0.8 and 1 with n_R=1, 2 and 4 and n_T=2.

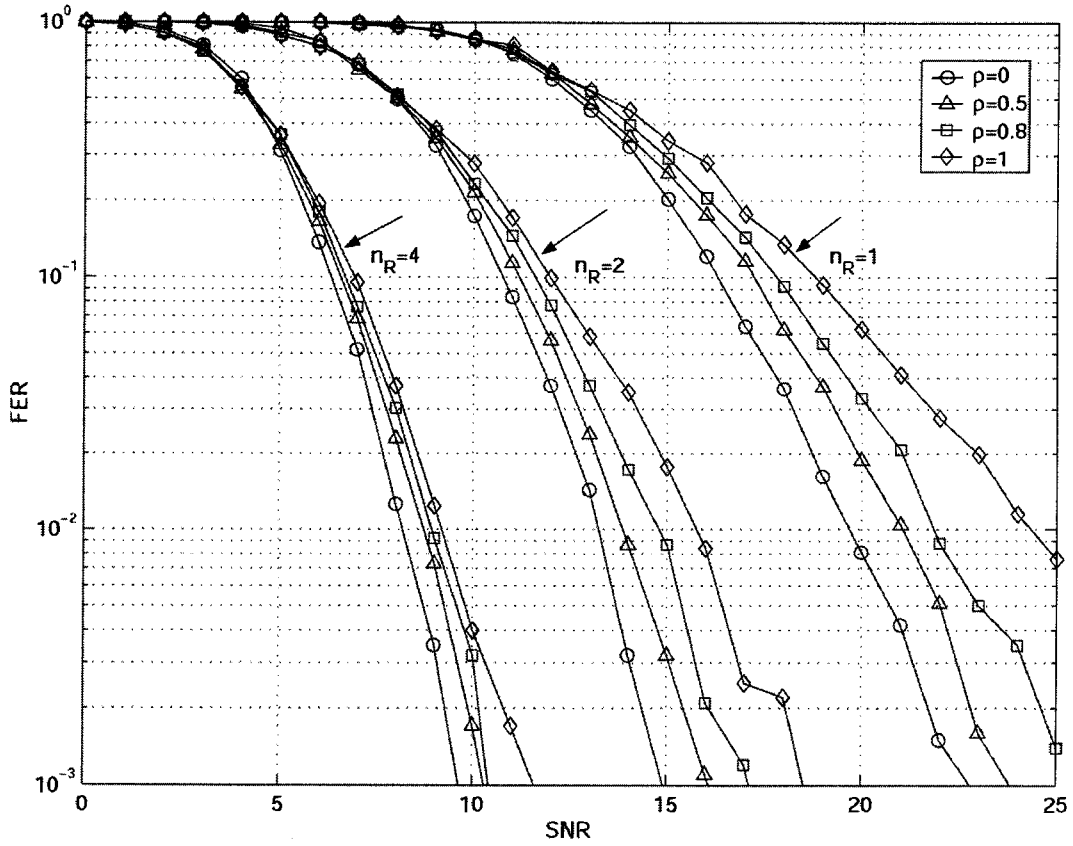

Figure 3.28: Performance Comparison of the 8-PSK 8-state STTCs from Table 1 over correlated Nakagami fading channels for ρ=0, 0.5, 0.8 and 1 with n_R=1, 2 and 4 and n_T=2.

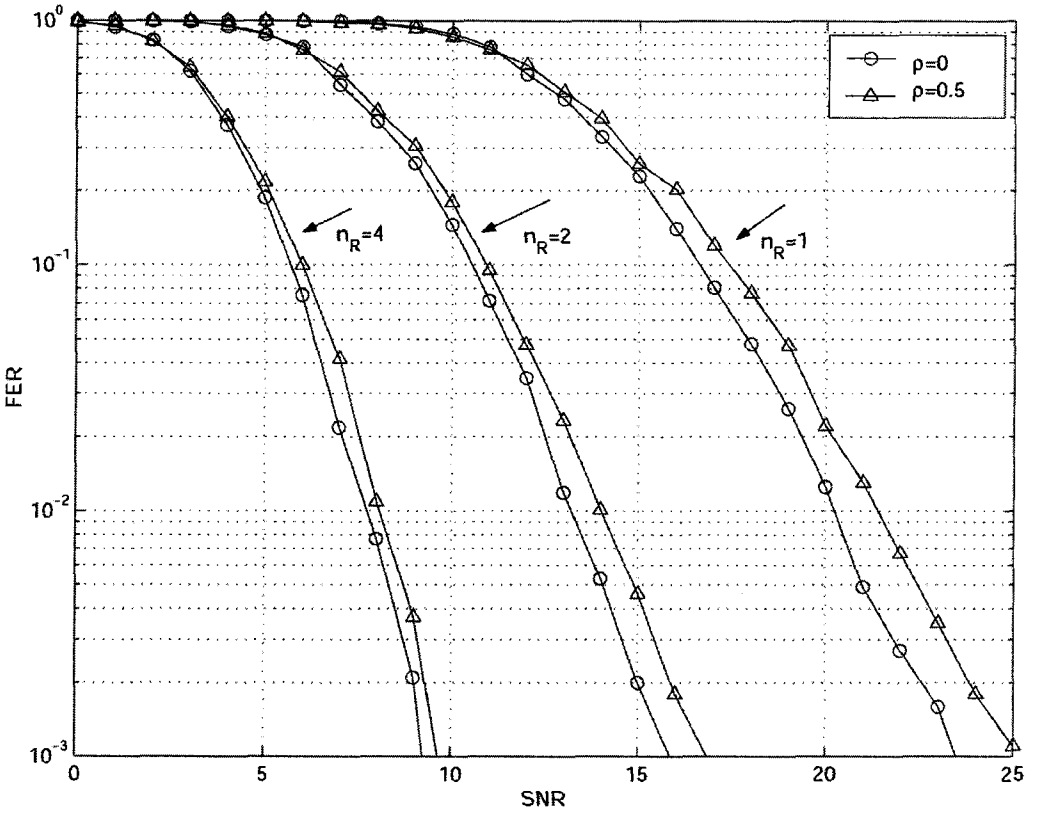

Figure 3.29: Performance Comparison of the 8-PSK 16-state STTCs from Table 1 over correlated Nakagami fading channels for ρ=0 and 0.5 with n_R=1, 2 and 4 and n_T=2.

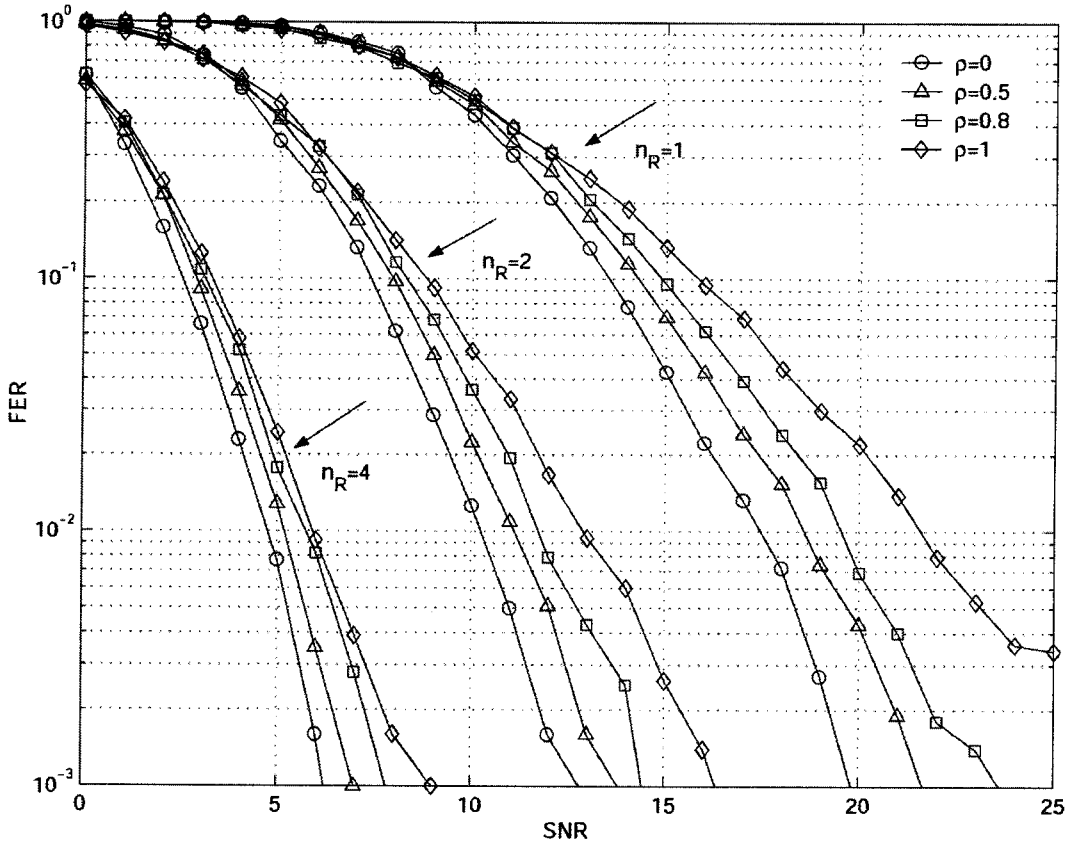

Figure 3.30: Performance comparison of the 4-PSK 4-state STTCs from Table 2 (Chen et al.) over correlated Nakagami fading channels for ρ =0, 0.5, 0.8 and 1 with n_R =1, 2 and 4 and n_T =2.

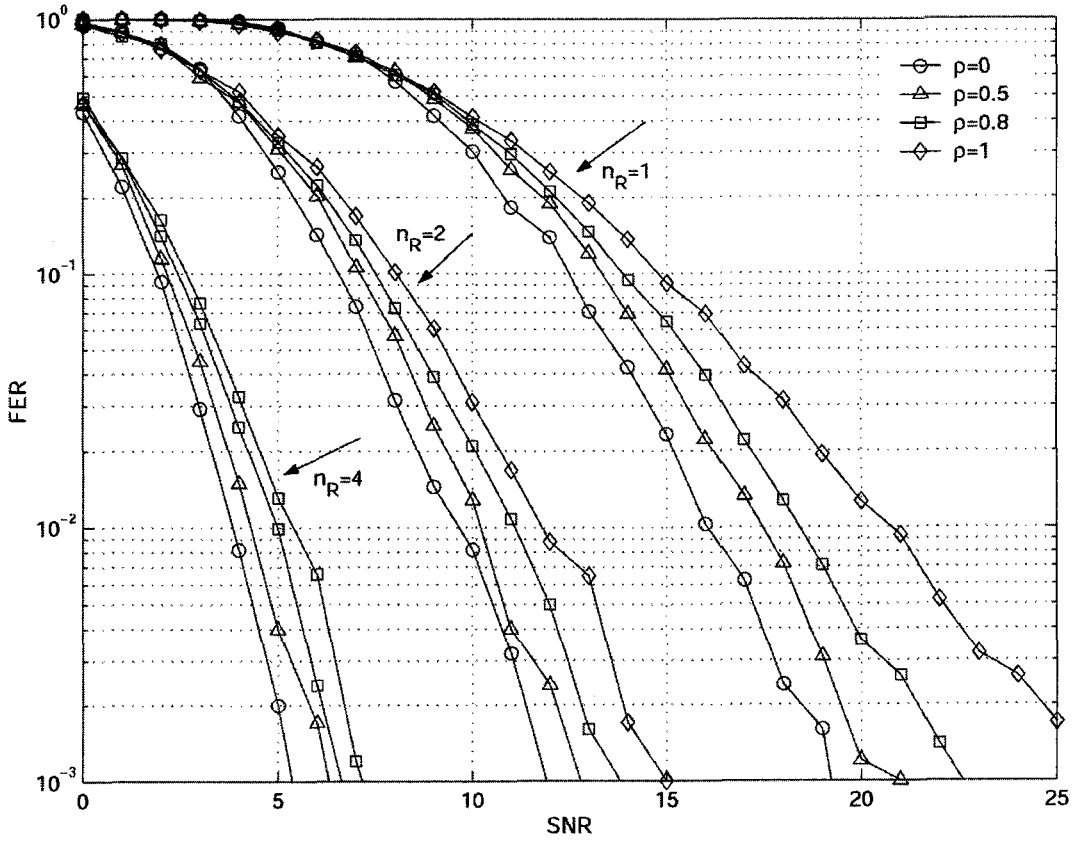

Figure 3.31: Performance Comparison of the 4-PSK 8-state STTCs from Table 2 (Chen et al.) over correlated Nakagami fading for ρ=0, 0.5, 0.8 and 1 with n_R=1, 2 and 4 and n_T=2.

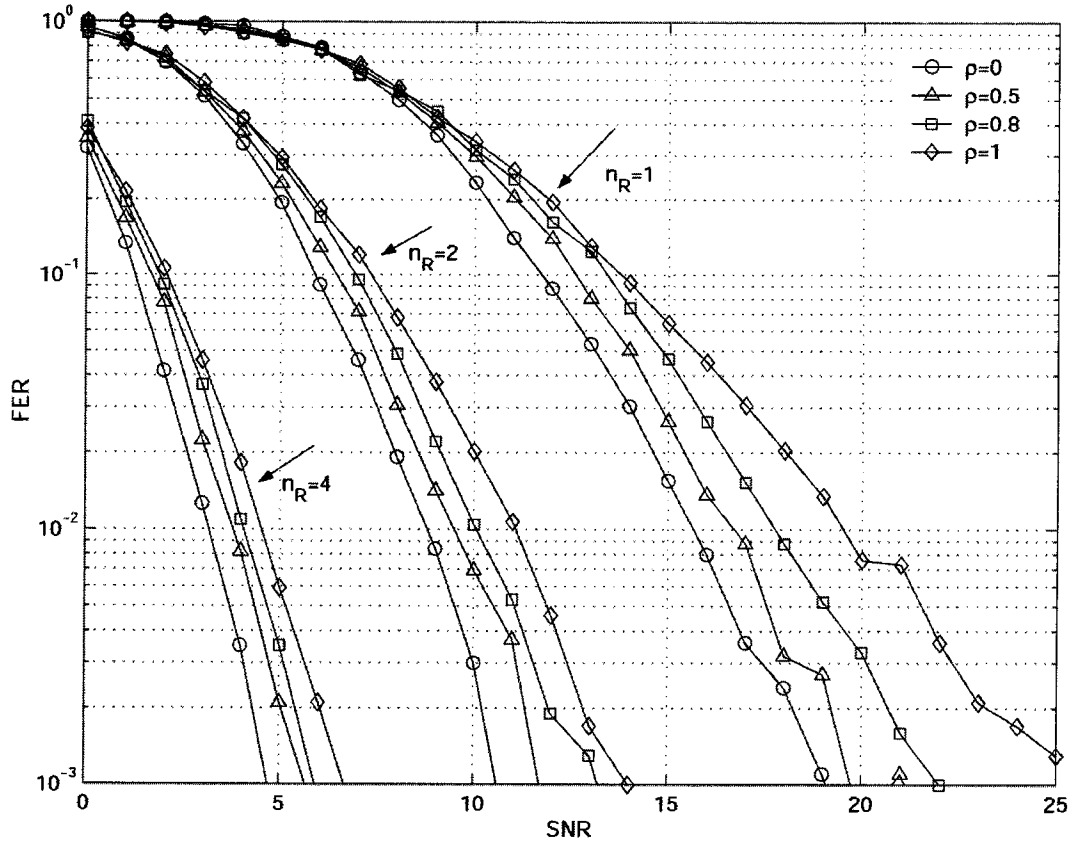

Figure 3.32: Performance Comparison of the 4-PSK 16-state STTC from Table 2 over correlated Nakagami fading channels for ρ=0, 0.5, 0.8 and 1 with n_R=1, 2 and 4 and n_T=2.

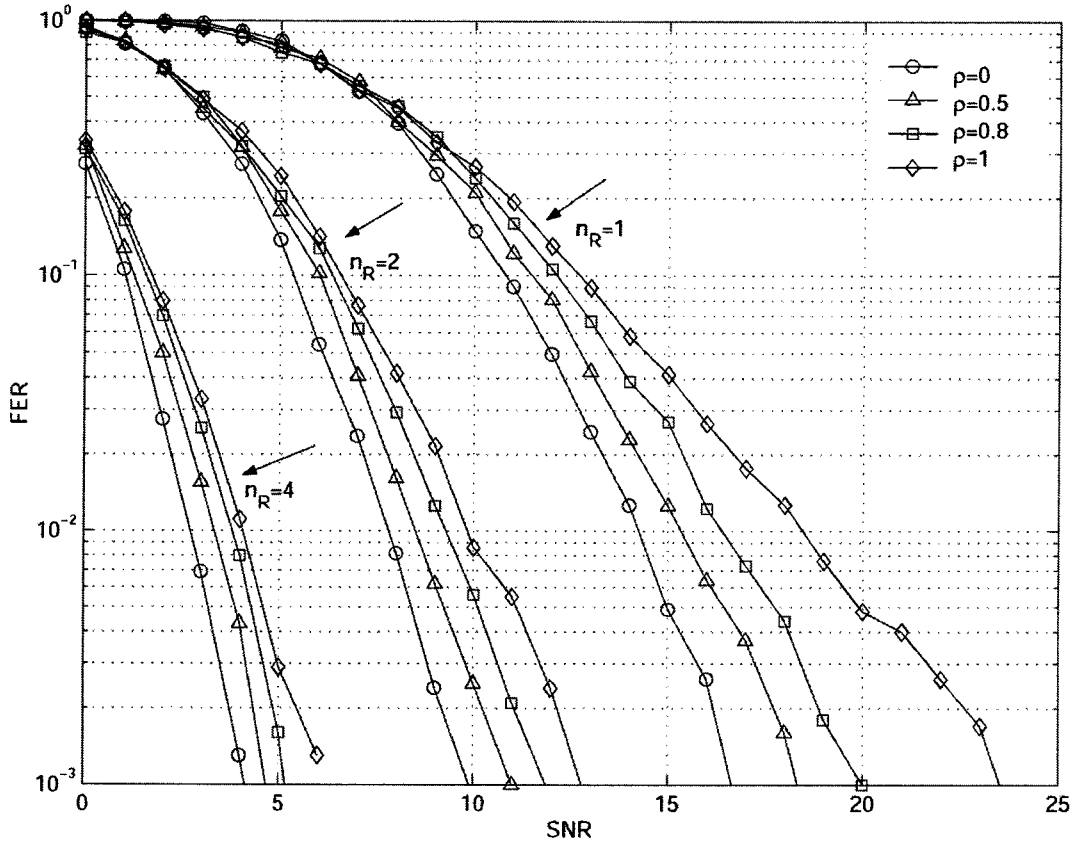

Figure 3.33: Performance Comparison of the 4 PSK 32-state STTC from Table 2 over correlated Nakagami fading channels for ρ=0, 0.5, 0.8 and 1 with n_R=1, 2 and 4 and n_T=2.

CHAPTER 4
CONCLUSION AND FUTURE WORK

In this chapter, an overview of the results is presented and possible extensions of the research on STTCs are discussed.

4.1 Summary

We have presented the evaluation and the performance of the Space-Time Trellis Codes (STTCs) proposed in [1], [2] and [19] over different fading channels. In [1], [2] and [19] a design criteria for STTCs was proposed and presented for Rayleigh fading channels. In [22] the performance of the STTCs of Table 1 (proposed by Tarokh et al. [1]) over independent and correlated Nakagami fading channels was presented. In this thesis we presented the performance of the STTCs in both Table 1 and Table 2 (Proposed by Chen et al. [12] and [19]) over Rayleigh, Ricean and Nakagami fading channels. We mainly focused on independent and correlated Nakagami fading channels.

In Chapter 2 we presented the theory of STTCs. We presented the performance analysis of STTCs over Rayleigh, Ricean and Nakagami fading channels [1], [12] and [19]. We discussed the space-time trellis code construction and design criteria in detail.

In Chapter 3 we presented the simulation results. From these results we found that the space-time code design criteria proposed for Rayleigh and Ricean fading channels is suitable for Nakagami fading channels. From Figures 3.7 and 3.8, we found that over Ricean fading channels, the STTCs in Table 2 outperform the STTCs in Table 1. From Figures 3.12 to 3.33 we found that the performance of the STTCs in Table 2 is better than the STTCs in Table 1 over Nakagami fading channels. It was reported in [19] for Rayleigh fading channels with a single receive antenna, that when n_T is increased from two to three and four, worse performance was degraded for the 4-PSK 4-state STTC in Table 2. In Figure 3.20 we observed that in a Nakagami fading channel, this code also perform worse with a single receive antenna, when n_T is increased from two to three and from three to four. Even when we used four receive antennas as shown in Figure 3.21, performance did not improve.

Except for this case we found that significant performance improvements can be achieved if we increase the number of transmit antennas from two to three and four. By increasing the number of transmit antennas at the base station a significant performance improvement can be achieved without increasing the burden of the receivers. In Section 3.4.2 we discussed correlated fading channels and found that this correlation may degrade performance. The codes in Table 2 showed good performance over correlated fading channels. For a system with a single receive antenna, performance was worse in correlated channels than the uncorrelated channels. However employing multiple receive antennas can reduce the effect of the channel correlation.

4.2 Future Work

In Section 3.4.2, we showed the effect of correlated fading channels. It is important to reduce the effect of the correlation, and this can be achieved in several ways. An interesting way to reduce the correlation is proposed in [64]. Here it is proposed to use two different base stations to transmit the STTC coded signal instead of transmitting from a single base station.

In [5] Tarokh et al. proposed a 16-state 16-QAM (Quadrature Amplitude Modulation) STTC. There has not been much work done in STTC design for QAM, so it will be interesting field for future research.

Another active area of research is the combination of space-time codes with orthogonal frequency division multiplexing (OFDM). For high data rate wireless applications OFDM is widely used because of its ability to combat intersymbol interference (ISI). In a recent work it was shown that the performance of OFDM systems could be improved using STBCs [66].

Another interesting topic that may be pursued in future work is iterative decoding for STTCs. In [53] [40], an iterative decoding technique for STTC was presented. They found that significant coding gains could be obtained, but at the cost of higher decoding complexity.

References

[1] G.L. Stuber, Principles of Mobile Communications. USA, Kluwer Academic Publishers, 2001.

[2] M. Nakagami, "The m-distribution: A general formula of intensity distribution of rapid fading," in *Statistical Methods in Radio Wave Propagation*, W. G. Hoffman, Ed. Oxford, England: Pergamon, 1960.

[3] Y. Gong and K. B. Letaief, "Performance of space-time trellis coding over Nakagami fading channels" IEEE *Vehic. Tech. Conf.*, pp. 1405-1409, Spring 2001.

[4] B. Sklar, Digital Communications Fundamentals and Applications, Second Edition, Upper Saddle River, NJ, Prentice Hall P T R, 2001.

[5] V. Tarokh, N. Seshadri, A. R. Calderbank, "Space-time codes for high data rate wireless communication: performance criterion and code construction," *IEEE Trans. Inform. Theory*, vol .44, pp. 744-65, Mar. 1998.

[6] V. Tarokh, N. Seshadri, A. R. Calderbank, "Space-time codes for high data rate wireless communication: performance criteria," *1997 IEEE Int. Conf. Communications*, vol.1, pp. 299-303,1997.

[7] A. F. Naguib, V. Tarokh, N. Seshadri, A. R. Calderbank, " A space-time coding modem for high-data-rate wireless communications," *IEEE J Select. Areas in Commun.*, vol. 16, no. 8, pp. 1459-78, Oct. 1998.

[8] A. F. Naguib, V. Tarokh, N. Seshadri, A. R. Calderbank, " Space-time coded modulation for high data rate wireless communications," *IEEE Global Telecommun Conf.*, vol. 1, pp. 102-109, 1997.

[9] N. Seshadri, V. Tarokh, A.R. Calderbank," Space-time codes for wireless communication: code construction," *IEEE 47th Vehic. Tech. Conf. Tech.*, pp. 637-641, 1997.

[10] V.Tarokh, H.Jafarkhani, and A.R.Calderbank, "Space–time block codes from orthogonal designs," *IEEE Trans. Inform. Theory*, vol. 45, pp. 1456–1467, July 1999.

[11] V. Tarokh, A.F. Naguib, N. Seshadri, A.R. Calderbank., "Space-time codes for high data rate wireless communication: performance criteria in the presence of channel estimation errors, mobility, and multiple paths," *IEEE Trans. Commun.*, vol. 47, pp. 199-207, Feb. 1999.

[12] S. M. Alamouti, "A simple transmitter diversity scheme for wireless communications," *IEEE J. Select. Areas Commun.*, vol. 16, pp. 1451–1458, Oct. 1998.

[13] A. Paulraj., R. Nabar and D. Gore, Introduction to Space-Time Wireless Communications, Cambridge, UK, Cambridge University Press, 2003.

[14] W. Su and X.G. Xia, "Two generalized complex orthogonal space-time block codes of rates 7/11 and 3/5 for 5 and 6 transmit antennas," *IEEE Trans. on Inform. Theory*, vol. 49, no. 1, Jan. 2003.

[15] D. Varshney, C. Arumugam, V. Vijayaraghavan, N. Vijay and S. Srikanth, "Space-time codes in wireless communications," *IEEE Potentials,* vol. 22, pp.36 – 38, August-September 2003.

[16] S. Baro, G. Bauch, A. Hansmann, "Improved codes for space-time trellis-coded modulation.," *IEEE Commun. Letters*, vol.4, no.1, pp.20-22 Jan. 2000

[17] D. M. Ionescu, "New results on space-time code design criteria" *IEEE Wireless Communications and Networking Conf.*, pp. 684-687, 1999.

[18] D. M. Ionescu, K. K. Mukkavilli, Y. Zhiyuan and J. Lilleberg, "Improved 8- and 16-state space-time codes for 4PSK with two transmit antennas," *IEEE Commun. Lett.*, vol. 5, no. 7, pp. 301-303, July 2001.

[19] Z. Chen, J. Yuan, B. Vucetic, "Improved space-time trellis coded modulation scheme on slow Rayleigh fading channels," *Electronics Lett.*, vol.37, pp.440-441, 29 Mar. 2001.

[20] Z. Chen, J. Yuan and B. Vucetic," An improved space-time trellis coded modulation scheme on slow Rayleigh fading channels," *IEEE International Conf. Commun.,* pp.1110-1116, 2001.

[21] Z. Chen, B. Vucetic, J. Yuan and Lo. Ka. Leong, "Space-time trellis codes for 4-PSK with three and four transmit antennas in quasi-static flat fading channels," *IEEE Commun. Lett.*, vol. 6, no. 2, pp. 67-69, Feb. 2002.

[22] J. Yuan, Z. Chen and B. Vucetic, " Performance of space-time coding on fading channels," *IEEE Trans. Commun* , vol. 51, no. 12, pp. 1991-1996, Dec. 2003.

[23] Q. T. Zhang, "A Decomposition Technique for Efficient Generation of Correlated Nakagami Fading Channels," *IEEE J. select. areas commun.*, vol. 18, no. 11, Nov. 2000.

[24] Q. Yan, R. S. Blum, "Optimum space-time convolutional codes," *IEEE Wireless Commun. and Networking Conf.*, vol.3, pp.1351-1355, 2000.

[25] H. Boleskei and A. J. Paulraj, "Performance of space-time codes in the presence of spatial fading correlation," *in Asilomar Conf. on Signals, Systems, and Computers*, 2000.

[26] S. Siwamogsatham and M. O. Fitz, "Robust space-time coding for correlated Rayleigh fading channels," *Proc. 38th Allerton Conf. on Commun., Control, and Computing*, 2000.

[27] B. Sklar, Digital Communications Fundamentals and Applications, Second Edition, Upper Saddle River, NJ, Prentice Hall P T R, 2001.

[28] S. Wicker, Error Control Systems for Digital Communication and Storage. USA, Prentice Hall, 1995.

[29] S. Lin and D. J. Costello Jr., Error Control Coding Fundamentals and Applications. USA, Prentice-Hall, 1983.
[30] S. Haykin, Communication Systems. Delhi, India, *John Wiley and Sons*, 4th edition, 2001

[31] N. Yuen, " Performance Analysis of Space-time Trellis codes," Master of Engineering report, University of British Columbia, April 2000.

[32] J. Zhang and P.M. Djuric, "Joint channel estimation and decoding of space-time trellis codes," *IEEE Signal Processing Workshop on Statistical Signal Processing*, pp. 559-562, 2001.

[33] Y. Xue and X. Zhu, " Per-survivor-processing based adaptive decoder for space-time trellis code," *Acta Electronica Sinica*, vol. 29, no. 10, pp. 1352-1355, Publisher: Chinese Inst. Electron, China, Oct. 2001.

[34] Y. Xue and Z. Xuelong, "A new soft-decision adaptive decoder for space-time trellis code," *IEEE Intern. Conf. Personal Wireless Commun. Conf. Proc.*, pp. 162-166, 2000.

[35] Y. Xue and Z. Xuelong, "PSP-based decoding for space-time trellis code," *IEEE Asia-Pacific Conf. on Circuits and Systems.Electronic Commun. Systems*, pp. 783-786, 2000.

[36] M. J. Heikkila, E. Majonen and J. Lilleberg, "Decoding and performance of space-time trellis codes in fading channels with intersymbol interference," *IEEE International Symposium on Personal Indoor and Mobile Radio Communications.*, vol. 1, pp. 490-494, 2000.

[37] Y. Xue and Z. Xuelong, "PSP decoder for space-time trellis code based on accelerated self-tuning LMS algorithm," *Electronics Lett.*, vol. 36, no. 17, pp. 1472-1474, 17 Aug. 2000.

[38] Timothy J. Peters and John W. Waterston, http://www.waterston.org/john/ee359/

[39] M.O. Farooq, W. Li and T.A. Gulliver, " A new cellular structure with Space-Time Trellis Code", *Workshop on Wireless Circuits and Systems* (WoWCAS), Vancouver, Canada, pp. 10-11, May 21-22, 2004.

[40] W. C.Y. Lee, Mobile Cellular Telecommunications Systems. USA, McGraw-Hill, 1989.

[41] C. Zhipei, W. Zhongfeng and K.K. Parhi, "Iterative decoding of space-time trellis codes and related implementation issues," *Conference Record of the Thirty-Fourth Asilomar Conf. Signals, Sys. Comp.*, vol. 1, pp. 562-566, 2000.